akirin is required for diakinesis bivalent structure and synaptonemal complex disassembly at meiotic prophase I

Amy M. Clemons[a], Heather M. Brockway[a,b,*], Yizhi Yin[a,*], Bhavatharini Kasinathan[a], Yaron S. Butterfield[c], Steven J. M. Jones[c], Monica P. Colaiácovo[d], and Sarit Smolikove[a,b]
[a]Department of Biology and [b]Interdisciplinary Program in Genetics, University of Iowa, Iowa City, IA 52242; [c]Genome Sciences Centre, BC Cancer Agency, Vancouver, BC V5Z 1L3, Canada; [d]Department of Genetics, Harvard Medical School, Boston, MA 02115

ABSTRACT **During meiosis, evolutionarily conserved mechanisms regulate chromosome remodeling, leading to the formation of a tight bivalent structure. This bivalent, a linked pair of homologous chromosomes, is essential for proper chromosome segregation in meiosis. The formation of a tight bivalent involves chromosome condensation and restructuring around the crossover. The synaptonemal complex (SC), which mediates homologous chromosome association before crossover formation, disassembles concurrently with increased condensation during bivalent remodeling. Both chromosome condensation and SC disassembly are likely critical steps in acquiring functional bivalent structure. The mechanisms controlling SC disassembly, however, remain unclear. Here we identify *akir-1* as a gene involved in key events of meiotic prophase I in *Caenorhabditis elegans*. AKIR-1 is a protein conserved among metazoans that lacks any previously known function in meiosis. We show that *akir-1* mutants exhibit severe meiotic defects in late prophase I, including improper disassembly of the SC and aberrant chromosome condensation, independently of the condensin complexes. These late-prophase defects then lead to aberrant reconfiguring of the bivalent. The meiotic divisions are delayed in *akir-1* mutants and are accompanied by lagging chromosomes. Our analysis therefore provides evidence for an important role of proper SC disassembly in configuring a functional bivalent structure.**

Monitoring Editor
Kerry S. Bloom
University of North Carolina

Received: Nov 30, 2012
Revised: Jan 16, 2013
Accepted: Jan 23, 2013

INTRODUCTION

Meiosis is a specialized cell division that leads to the formation of haploid gametes, which in metazoans are the sperm and egg cells. It involves two cellular divisions after one cycle of replication; in the first (MI), homologous chromosomes segregate away from each other, and in the second (MII), sister chromatids separate (Figure 1A). During meiotic prophase I—the period preceding the first meiotic division—chromosomes are organized in the form of bivalents: pairs of homologous chromosomes connected by crossovers and sister chromatid cohesion. Proper bivalent structure is crucial for accurate meiotic division, and defects in its formation lead to improper chromosome segregation, embryonic lethality, and/or birth defects (Hassold and Hunt, 2001). Thus an elaborate sequence of events must be orchestrated to form a functional bivalent, which includes two major processes occurring in meiotic prophase I: the establishment of crossovers (early events) and the restructuring of the bivalent to form a compact structure (mid to late prophase I).

In most organisms, the formation of at least one crossover event per bivalent necessitates each chromosome finding its partner (pairing) and tightly associating with it (synapsing) via the synaptonemal complex (SC). The SC is a widely conserved protein structure

This article was published online ahead of print in MBoC in Press (http://www.molbiolcell.org/cgi/doi/10.1091/mbc.E12-11-0841) on January 30, 2013.

*These authors contributed equally.

Address correspondence to: Sarit Smolikove (sarit-smolikove@uiowa.edu).

Abbreviation used:SC, synaptonemal complex.

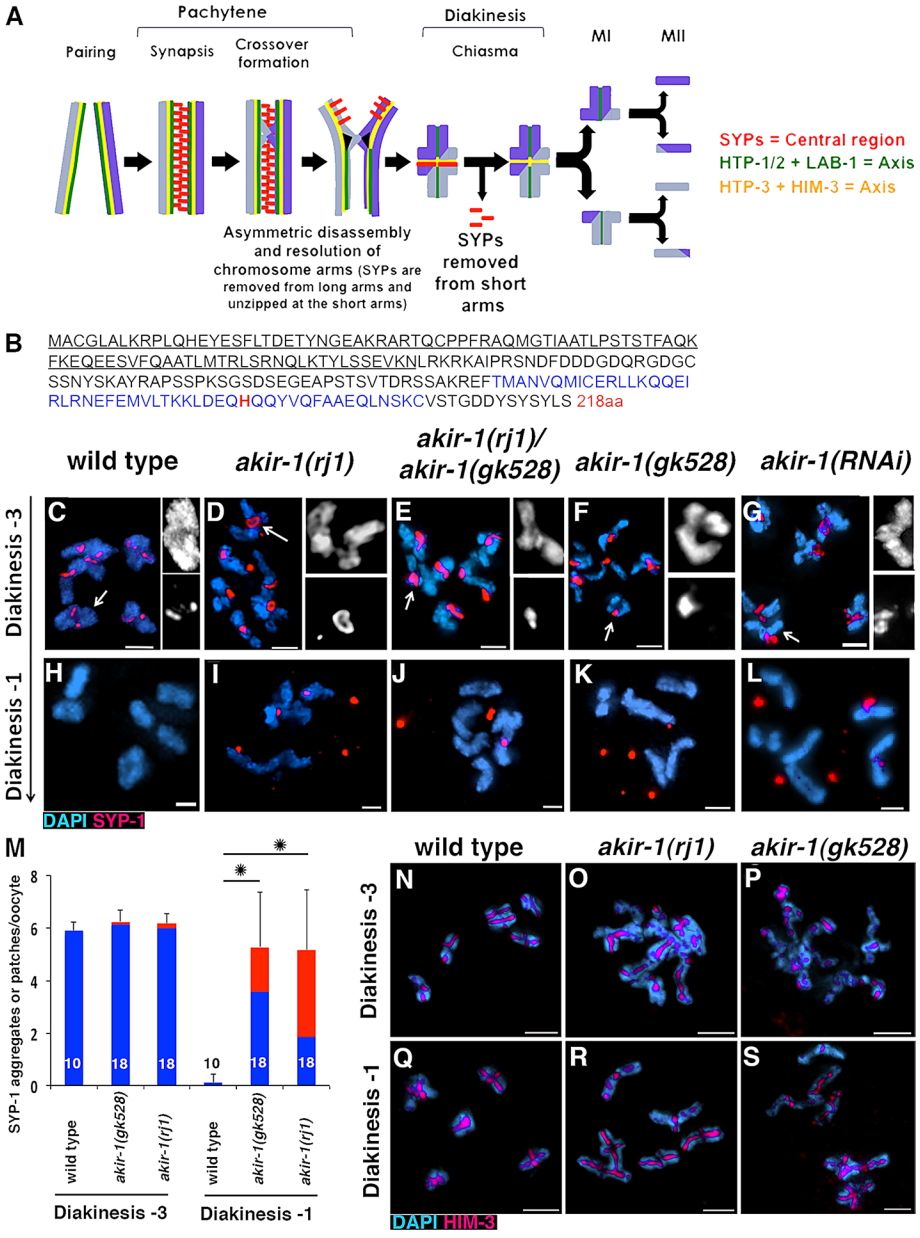

FIGURE 1: SC disassembly defects observed in *akir-1* mutants are specific to central region proteins. (A) Schematic representation of chromosome behavior in meiosis, highlighting key events in SC disassembly. Chromosomes are in blue. Central region proteins /SYPs are in red, and axis and axis-associated proteins are in green and yellow. (B) Schematic representation of the predicted AKIR-1 protein. The α-helical domain is in blue. The region of the protein deleted in the *gk528* mutant allele is indicated (underlined amino acids 1–91, 42% of the protein). Half of the predicted promoter is also removed by *gk528* but is not shown here. The red letter H indicates the position of the histidine mutated to proline in the *rj1* allele. (C–L) *akir-1* mutants exhibit aggregation of SYP-1, atypical bivalent structure (D–G, inset), and persistence of SYP-1 in diakinesis –1 (H–L). *akir-1(rj1)* and *akir-1(gk528)* alleles do not complement each other (E, J). Arrows in C–G point to the regions enlarged in the inset. Insets show separate channels: top, DAPI; bottom, SYP-1. (M) Number of SYP-1 aggregates or patches per oocyte associated with chromosomes (blue) or not associated with chromosomes (red) at diakinesis –1 and diakinesis –3. At diakinesis –3 almost all wild-type diakinesis bivalents associate with SYP-1, found as a patch in the short-arm region. *akir-1* mutants at this stage exhibit similar levels of association of SYP-1 aggregates with chromosomes (Fisher's exact test, $p = 0.49$, $p = 0.59$). At diakinesis –1 almost all wild-type diakinesis bivalents lack SYP-1, whereas *akir-1* mutants oocyte still contain approximately five SYP-1 aggregates (Fisher's exact test, $p < 0.001$), many of which still associated with chromosomes. The *n* values for number of oocytes scored are indicated on the graph. Error bars are SD, and statistically significant values (Mann–Whitney test, $p << 0.001$) are indicated with asterisk. (N–S) High-magnification images of DAPI- and HIM-3–stained nuclei of gonads. High-magnification images of DAPI-stained (blue) and SYP-1– (red, C–L) or HIM-3–stained (red, N–S) nuclei of gonads from age-matched wild type (C, H, N, Q), *akir-1(rj1)* (D, I, O, R), *akir-1(rj1)/akir-1(gk528)* (E, J), *akir-1(gk528)* (F, K, P, S), and *akir-1(RNAi)* (G, L) at diakinesis –3 (C–G, N–P) and diakinesis –1 (H–L, Q–S). Images are full projections of a single nucleus. Bars, 2 μm.

that physically connects homologous chromosomes in meiotic prophase I to mediate synapsis (Zickler and Kleckner, 1999). The SC is composed of two lateral elements (composed of axis-associated proteins) connected by central region proteins that form a zipper-like structure. This results in a tripartite complex that holds homologous chromosomes together until crossovers are formed. Crossovers then trigger SC disassembly along with condensation, which allows the visual manifestation of the crossover event—the chiasma (Schvarzstein *et al.*, 2010). Thus the SC is a prerequisite for functional bivalent formation; however, it is unclear whether this is due simply to the requirement for synapsis in general or whether the SC and its regulated disassembly directly affect bivalent structure.

In *Caenorhabditis elegans* late meiotic prophase I, each bivalent is reconfigured around the single off-centered crossover as an asymmetric cruciform structure, containing long and short arms (Schvarzstein *et al.*, 2010). The short arms of the bivalent are the sites at which connections between homologous chromosomes will be removed at MI (Rogers *et al.*, 2002), whereas the long arms maintain associations between sister chromatids until the onset of MII. Thus proper chromosome segregation relies on the restructuring of chromosomes into an asymmetric and tightly condensed cruciform structure. In *C. elegans*, the most significant condensation occurs during mid to late prophase. Of the three condensin complexes (condensin I^{DC}, condensin I, and condensin II), only the condensin II complex is required for the remodeling of the bivalent into the cruciform structure (Chan *et al.*, 2004). Although chromosome condensation and disassembly of the SC occur concurrently, it was shown that these two processes are independent of each other in *C. elegans* (MacQueen *et al.*, 2002; Colaiacovo *et al.*, 2003; Chan *et al.*, 2004; Smolikov *et al.*, 2007, 2009). Thus any effect SC disassembly might have on the organization of the bivalent is condensin independent. However, it has not been fully tested whether aberrant SC disassembly has implications for bivalent

structure, as known mutants affecting this process affect only a few of its aspects (Ivanovska *et al.*, 2005; Malmanche *et al.*, 2007; Bhalla *et al.*, 2008; de Carvalho *et al.*, 2008; Martinez-Perez *et al.*, 2008; Sourirajan and Lichten, 2008; Jordan *et al.*, 2009; Peretz *et al.*, 2009; Resnick *et al.*, 2009). This includes mutants affecting the timing of disassembly or altering the subchromosomal pattern of SC proteins, none of which perturb SC function by retaining its ability to connect homologous chromosomes.

To identify new players in chromosome behavior in meiosis, we performed a forward genetic screen in *C. elegans*, using SC disassembly defects as a functional readout. We identified AKIR-1, a novel *C. elegans* orthologue of fly and mouse *Akirins*, a gene family with no previously described role in meiosis. Here we present data suggesting that AKIR-1 supports the efficient removal of SC proteins from the chromosomes. In *akir-1* mutants, early meiotic events such as SC assembly and crossover formation occur normally. However, late prophase I events such as SC disassembly, chromosome condensation, and bivalent restructuring are severely perturbed. We show that *akir-1* is required to form a compact, cruciform-shaped bivalent structure and acts in both SC-dependent and SC-independent manners to influence chromosome behavior. Thus the *akir-1* phenotype shows that aberrant accumulation of SC proteins on chromosomes is linked to disrupted bivalent structure and perturbed meiotic divisions. Together, these data 1) identify the first known role for an *akirin* gene in meiosis in any organism, 2) indicate a new link between SC disassembly and chromosome structure in meiosis, and 3) suggest that regulated mechanisms exist to prevent aberrant accumulation of SC proteins after their removal from chromosomes during SC disassembly.

RESULTS

Isolation of the worm orthologue of *akirin*

We isolated *akir-1(rj1)* in a forward genetic screen aimed at identifying mutants that exhibit defects in SC disassembly (see *Materials and Methods*). Using a combination of single-nucleotide polymorphism (SNP) mapping (Davis *et al.*, 2005) and genome-wide sequencing techniques, we found that *rj1* resulted in a missense mutation (H190P) in E01A2.6. This is an uncharacterized open reading frame (ORF) that is germline expressed (Wang *et al.*, 2009), encoding a protein of 218 amino acids that lacks any known domains (Figure 1B) but is evolutionarily conserved among metazoans. We named E01A2.6 *akir-1* to adhere to the nomenclature established in other species (AKIRIN; Macqueen and Johnston, 2009). AKIR-1 has one orthologue in *Drosophila*, which is 31% identical and 47% similar to the *C. elegans* protein (MN168211). Vertebrates have two *akirin* genes, the protein products of which both share homology to the worm protein (~30% identity and ~50% similarity; MN001007589, BC082305). The analysis presented here is focused on the meiotic role of worm *akirin* and does not exclude mitotic or somatic functions for this gene, which are not examined here.

Mutation of worm *akirin* resulted in two phenotypes apparent in late meiotic prophase I: 1) failure in the timely removal of SC proteins from chromosomes, leading to their aggregation, and 2) delay in the condensation of chromosomes (Figure 1, D–G and I–L; diakinesis –3 and –1 are the third and first oocytes, respectively, before conclusion of meiotic prophase I). Both of these phenotypes are associated with an aberrant bivalent structure found in these mutants (Figure 1, D–G, inset). These defects were observed in every gonad dissected from worms containing either one of two *akir-1* alleles—*rj1* (the point mutant isolated in our screen) and *gk528* (a deletion mutant, obtained from the *C. elegans* Gene Knockout Consortium, Oklahoma Medical Research Foundation)—as well as in 91% of gonads ($n = 87$) dissected from *akir-1(RNAi)* worms. The *akir-1(rj1)* allele contains a histidine to proline substitution in position 190 (Figure 1B). This substitution is expected to result in a severe conformational change by disrupting the predicted α-helical structure of this conserved region (Cole *et al.*, 2008). The *akir-1(gk528)* deletion removes most of the promoter and coding sequence and is therefore expected to be a null. The molecular nature of the two alleles, their phenotypic similarity, and their phenocopy by RNA interference (RNAi) suggest that they are both loss-of-function alleles.

akir-1 mutants exhibit embryonic lethality that is maternally contributed

Both *akir-1* alleles exhibit moderate levels of embryonic lethality (Supplemental Table S1, 21% in *akir-1(rj1)* and 16% in *akir-1(gk528)* mutants; $p << 0.001$, Fisher's exact test). We also observed a modest increase in the number of males (0.6% in *akir-1(rj1)* and 0.9% in *akir-1(gk528)*, compared with <0.2% in wild type, significant for *akir-1(gk528)*, $p = 0.009$, Fisher's exact test). The contribution to embryonic lethality is maternal, as *akir-1(gk528)* or *akir-1(gk528); fem-2(b245)* mated to wild-type males show similar levels of embryonic lethality to that observed in self-progeny of the hermaphrodite *akir-1(gk528)* (Supplemental Table S1, $p = 0.34$, $p = 0.19$, Fisher's exact test). Whereas early meiotic events (such as pairing, synapsis, and recombination) are similar in males and females, late meiotic events (such as apoptosis, chromosome condensation, and SC disassembly) are differentially regulated in the two sexes of *C. elegans* (Shakes *et al.*, 2009). Moreover oocytes, but not sperm, are loaded with maternally contributed proteins, some of which are crucial for development. All of these may account for the maternally contributed embryonic lethal phenotype of *akir-1* mutants. We also found a reduction in the number of eggs laid (eggs per worm [average ± SD]: wild type, 256 ± 45; *akir-1(rj1)*, 46 ± 22; *akir-1(gk528)* 75 ± 24), which is also maternally contributed.

akir-1 is required for the removal of central region proteins, but not lateral element/axis proteins, from chromosomes

SC proteins begin to load onto wild-type chromosomes at the entrance to meiotic prophase I (transition zone: leptotene–zygotene), and by the pachytene stage the SC is fully assembled between homologous chromosomes (for model, see Figure 1A). The process of SC assembly was not affected in the *akir-1* mutants (Supplemental Figure S1, F–H). Moreover, *akir-1* mutants exhibited no defects in entering meiotic prophase I, as indicated by the wild-type clustered morphology of chromosomes and their nuclear organization (Supplemental Figures S1, F–H, and S2A). Pachytene chromosomes of *akir-1* mutants exhibited aligned parallel tracks, indicative of synapsis, throughout pachytene, as observed in wild type (Supplemental Figures S1, J–L, and S3). In late pachytene, when SC disassembly initiates, some SC regions appeared thickened in *akir-1* mutants (Supplemental Figure S1, N–P). However, a clear meiotic defect became evident only in oocytes at diakinesis, the last stage of meiotic prophase I. Therefore, although the origin of the defects is likely to be in late pachytene, for most of our analysis of SC disassembly we focused on –3 and –1 diakinesis oocytes (indicated in Supplemental Figure S2A).

An oocyte at diakinesis –3 is the third oocyte before fertilization/conclusion of meiotic prophase I; this is the last oocyte in which central region (SYP) proteins are found on chromosomes in the wild-type gonad (total of six patches, one per diakinesis bivalent; Figure 1M; Nabeshima *et al.*, 2005). *akir-1* mutants contained on average approximately six SYP-1 signals, matching the number of chromosome pairs and SYP-1 patches in wild-type nuclei (Figure 1M).

However, SYP-1 proteins exhibited aggregated localization (Figure 1, D–G). Quantification of SYP-1 signal intensity suggested that these aggregates contain almost triple the amount of SYP-1 protein observed in wild-type cells (2.9 times SYP-1 signal increase: wild type, *akir-1(rj1)*, $n = 24$, 42 patches/aggregates, $p < 0.001$ by the two-tailed Mann–Whitney test, 95% confidence interval). Diakinesis –1 is the position of the last oocyte before fertilization/conclusion of meiotic prophase I, and in wild-type gonads this oocyte consistently lacks any central region/SYP staining (Figure 1H; Nabeshima *et al.*, 2005). Remarkably, SYP-1 disassociation from chromosomes was delayed in *akir-1* mutants, as SYP-1 was still present in all diakinesis –1 nuclei although absent from wild-type nuclei (Figure 1, H–L). A large fraction of these aggregates was found to associate with chromosomes (Figure 1M, blue). The extended localization of SYP proteins into diakinesis –1, as well as their aggregation, indicated defects in the removal of SC proteins from chromosomes in *akir-1* mutants.

Overall, fewer nuclei were at the stage of diakinesis in *akir-1* mutants compared with wild type (wild type, 8.3 ± 1.6; *akir-1(rj1)*, 3.6 ± 1; *akir-1(gk528)*, 6.3 ± 1.6; $n = 111$, 30, 101 gonads, $p < 0.001$ for both, Mann–Whitney test). This also correlated with a decrease in the overall size of the gonad in *akir-1* mutants (Supplemental Figure S2). Of importance, the reduced number of diakinesis nuclei does not contribute to the germline phenotypes discussed here (SC disassembly, condensation, and bivalent structure) because other mutants that exhibit reduced numbers of diakinesis nuclei still show wild-type chromosome structure at diakinesis and normal SC disassembly (Supplemental Figure S4). Hence, although we cannot fully rule out the possibility that the reduced number of diakinesis nuclei is a result of slower progression of meiosis in *akir-1* mutants (which is specific to the diplotene–diakinesis stage), it is likely not causal to the phenotypes described here. Moreover, the effect of *akir-1* on meiosis is unlikely to be due to transcriptional changes of SYP-1, as SYP-1 mRNA levels are not altered in *akir-1* mutants (levels normalized to *myo-3* control: wild type, 0.89±0.01, and *akir-1(rj1)*, 0.87 ± 0.02 [average ± SD]. This is consistent with the established findings that germline genes are translationally regulated (Merritt *et al.*, 2008) and that transcription is repressed in late meiotic prophase I in *C. elegans* (Walker *et al.*, 2007), the stage in which the *akir-1* mutant phenotypes are observed.

The central region of the SC in *C. elegans* is composed of four SYP proteins, which exhibit similar localization patterns, interdependent localization, and indistinguishable phenotypes of null mutants (MacQueen *et al.*, 2002; Colaiacovo *et al.*, 2003; Smolikov *et al.*, 2007, 2009). In addition to the SYPs, five axis-associated proteins (HIM-3, HTP-3, HTP-1/2, and LAB-1) localize to the SC throughout meiotic prophase I. By light microscopy, axis-associated proteins exhibit similar localization patterns to central region proteins during pachytene. We hypothesized that the *akir-1* mutant would exhibit similar defects in SC disassembly for all four SYP proteins but that loss of AKIR-1 might not disrupt other SC proteins. Indeed, the localization of SYP-2, SYP-3, and SYP-4 showed aggregation upon SC disassembly, identical to that observed for SYP-1 (Supplemental Figure S5 and unpublished data). Costaining with antibodies against SYP-1 and SYP-3 revealed that both colocalized to the same aggregates in the *akir-1(rj1)* mutant (Supplemental Figure S5, M–O). Therefore, all central region proteins mislocalize in *akir-1* mutants in a similar manner and are likely to associate with each other in the same aggregate. Unlike central region proteins, the localization of axis-associated proteins in *akir-1* mutants was indistinguishable from wild type in both the timing and the pattern of localization. Axis-associated proteins were distributed linearly along the arms of the diakinesis bivalent in *akir-1* mutants, unlike the aggregated localization of the SYPs; HIM-3 and HTP-3 associated with both diakinesis bivalent arms (Figure 1, O–P, R, and S, and unpublished data), and LAB-1 and HTP-1/2 (Figure 2, B and D, and unpublished data) associated exclusively with the long arm of the diakinesis bivalent. Thus aberrant SC protein localization is limited to the central region proteins in *akir-1* mutants.

AKIR-1 is required for short-arm resolution

A wild-type SC structure, before its disassembly, contains a tripartite organization: SYPs flanked by axial proteins, where SYPs serve as axial connectors (Schild-Prüfert *et al.*, 2011). In *C. elegans,* disassembly of the SYPs from the short versus the long arm of the bivalent is asymmetric (Nabeshima *et al.*, 2005). SYPs are promptly removed from the long arm upon initiation of SC disassembly starting at late pachytene, whereas they remain associated with the short arm until the transition to diakinesis –1 (for model, see Figure 1A). This progressive asymmetric disassembly process is proposed to secure the resolution of all four chromosomal arms and the formation of a cruciform bivalent.

We examined whether the defects in the disassembly of the SYPs are specific to the short and/or the long arm of the bivalent in *akir-1* mutants. After crossover formation, SYP proteins no longer localize along the long arm of the bivalent, whereas LAB-1 and HTP1/2 are retained at this location. Conversely, SYP proteins remain associated along the short arm, whereas LAB-1 and HTP1/2 are no longer associated with this region of the bivalent (de Carvalho *et al.*, 2008; Martinez-Perez *et al.*, 2008). If SYPs were properly removed from the long arm of the bivalent in *akir-1* mutants, we would expect that 1) SYP-1 and LAB-1 would localize to distinct domains, and 2) SYP-1 would localize terminally to a crossover marker (since crossovers mark the boarders of the LAB-1/SYP-1 domains at this stage). We found that, as in wild type, SYP-1 and LAB-1 do not colocalize in diakinesis in *akir-1* mutants (Figure 2, B and D). Moreover, SYP-1 aggregates acquired terminal (92% of foci, $n = 66$; Figure 2, F–F′) rather than central positioning relative to a crossover marker (ZHP-3, the *C. elegans* orthologue of the yeast ZIP3, marks crossovers cytologically, forming one focus on each diakinesis bivalent; Jantsch *et al.*, 2004; Bhalla *et al.*, 2008). This indicates that SYP-1 localization is restricted to one side of the crossover normally in *akir-1* mutants, which suggests that AKIR-1 is dispensable for removal of SYPs from the long arm of the bivalent.

Analysis of SYP-1 and HIM-3 localization along the short arm of the bivalents revealed that whereas in wild type, SYP-1 localization is no longer observed on this chromosome domain in late diakinesis, the HIM-3 signal is observed overlapping with the borders of the SYP-1 aggregate in 94% of the *akir-1*–mutant diakinesis bivalents ($n = 66$; Figure 2G). Thus we hypothesize that in *akir-1* mutants SYPs may persist in connecting homologous chromosomes beyond the normal point of SC disassembly, therefore perturbing short-arm resolution.

To examine this hypothesis, we tested whether SYP-1 aggregates were capable of connecting chromosomes in a scenario in which other means of chromosomal association, such as crossovers, were absent. SPO-11 is required for the generation of meiosis-specific double strand breaks (DSBs) and therefore for crossover formation (Dernburg *et al.*, 1998). Its absence results in patchy localization of SYP-1 on the 12 univalents formed, with no restriction to a particular side of the chromosome (Nabeshima *et al.*, 2005; Figure 2I). *akir-1(RNAi)* in the *spo-11(ok79)* mutant genetic background resulted in formation of SYP-1 aggregates (Figure 2, K and O). These SYP-1 aggregates in *akir-1(RNAi); spo-11(ok79)* mutants were

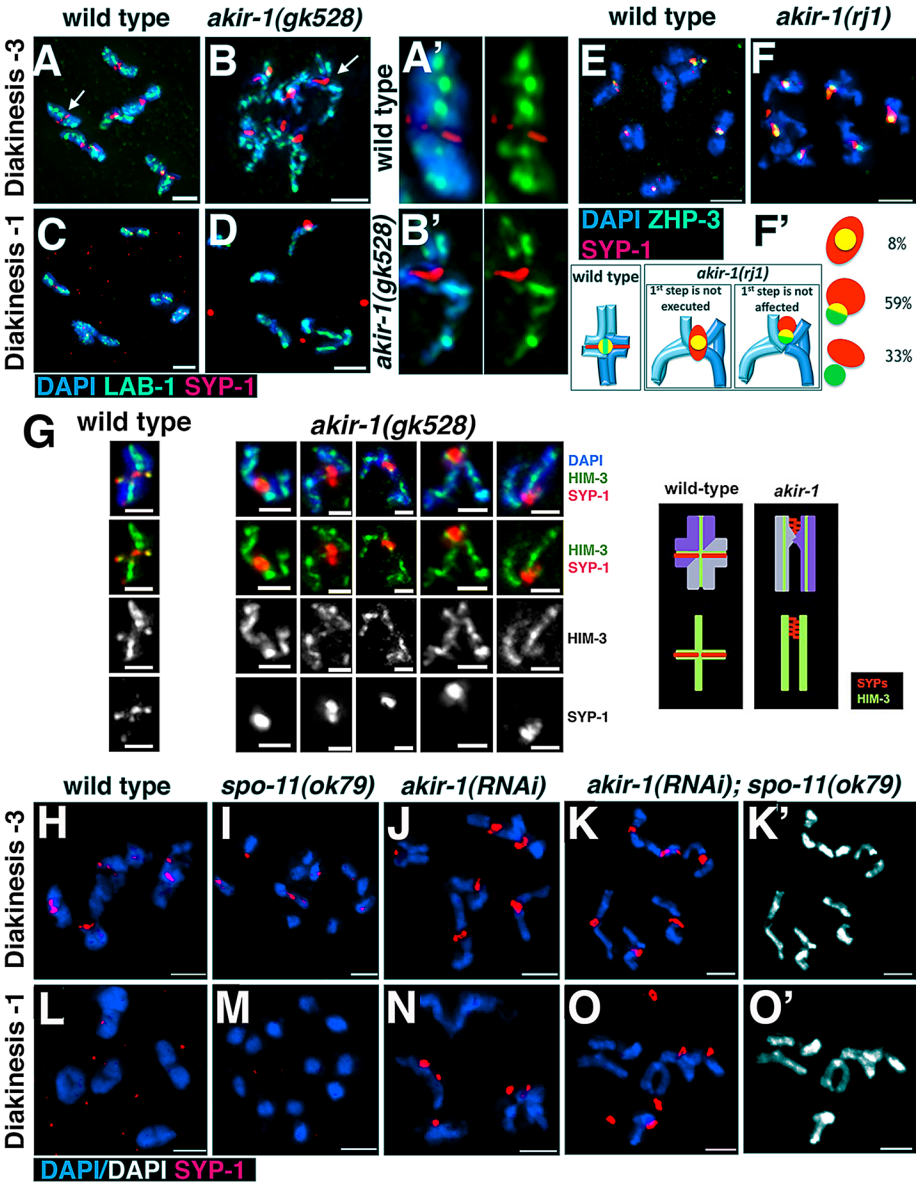

FIGURE 2: In *akir-1* mutants, SC disassembles aberrantly from the short arm of the bivalent, whereas the long arm is not affected. (A–D) Central region and axis-associated proteins do not colocalize in *akir-1* mutants. (E–F′) Central region proteins are localized terminally to a marker for crossover site. (G) Tripartite SC in *akir-1* mutant diakinesis bivalents. Right, schematic representation of the images. (H–O′) SYP-1 aggregates are present in crossover-deficient backgrounds that lack AKIR-1. These aggregates associate pairs of univalents. DAPI-only channels (K′, O′) show lack of chiasma between the univalents connected by the SYP-1 aggregate. High-magnification images of nuclei of gonads from age-matched wild type (A, A′, C, E, G left, H, L), *akir-1(rj1)* mutants (F), *akir-1(gk528)* mutants (B, B′, D, G right), *akir-1(RNAi)* (J, N), *spo-11(ok79)* (I, M), and *akir-1(RNAi); spo-11(ok79)* (K, K′, O, O′) adult hermaphrodites at diakinesis –3 (A–B′, E–G, H–K′) and diakinesis –1 (C, D, L–O′). All gonads were stained with DAPI (blue or white) and SYP-1 (red). Those in A–D were stained with LAB-1 (green), those in G with HIM-3 (green or white), and those in E and F contained GFP::ZHP-3 fusion protein (green). A′ and B′ are zoomed-in images of the chromosomes marked by an arrow in A and B (all three channels on the left; antibody-only channel on the right). (F′) Quantitative analysis of the various types of localization patterns observed in *akir-1(rj1)* mutants for ZHP-3 (green) and SYP-1 (red). Images are full projections of a single nucleus (A–F, H–O′) or a single bivalent (G). Bars, 1 μm (G), 2 μm (A–F, H–O′).

frequently found between pairs of chromosomes (Figure 2, K and O); these interchromosomal aggregates significantly decreased the distance between 4′,6-diamidino-2-phenylindole (DAPI) bodies (almost twofold at diakinesis –3; see Table 1 for data and Supplemental Table S2 for statistics). This chromosomal association is dependent on the presence of an aggregate, as 1) chromatin (DAPI stained) bridges were not observed between pairs of chromosomes (Figure 2, K′ and O′; the space occupied by the aggregates connecting the bivalents does not contain chromatin); 2) the frequency of associations was reduced as chromosomes progressed through meiosis and aggregates disassociated from chromosomes (percentage of nuclei with aggregation: 85% of diakinesis –3 nuclei, $n = 26$; 37% of diakinesis –1 nuclei, $n = 27$; $p < 0.001$, Fisher's exact test); and 3) the association was dependent on the presence of SYP proteins (*akir-1(RNAi); syp-2(ok307); spo-11(ok79)* interchromosomal distances were larger than that of *akir-1(RNAi); spo-11(ok79)* mutants and indistinguishable from that of *syp-2(ok307)* and *spo-11(ok79)* single or double mutants (see Table 1 for data and Supplemental Table S2 for statistics). Thus, in *akir-1* mutants, SYP-1 aggregates represent a form of SC that retains the property of connecting homologous chromosomes at a stage when this attribute is lost from wild-type oocytes. Of interest, in some species the SC can substitute for lack of chiasmata throughout meiosis, similarly to what is found in *akir-1(RNAi); spo-11(ok79)* mutants in the diakinesis stage (de la Fuente *et al.*, 2012). These data are consistent with a role for AKIR-1 in the resolution of the short arms of the bivalent, in addition to its role in the timely removal of SC proteins from chromosomes.

AKIR-1 is not involved in chromosome pairing or crossover formation

HTP-1 and -2 affect chromosome pairing in addition to their role in promoting proper SC disassembly (de Carvalho *et al.*, 2008; Martinez-Perez *et al.*, 2008). Therefore, we tested whether AKIR-1 is involved in chromosome pairing during meiotic prophase I. To examine the progression of homologous chromosome pairing, we performed fluorescence in situ hybridization (FISH) for the 5S locus (a central position on chromosome V). Pairing in both wild type and *akir-1* mutants was initiated as nuclei entered meiosis (zone 3, transition zone), peaked as nuclei progressed to the pachytene region (zone 4), and was maintained at high levels throughout meiotic prophase I (Figure 3H). There was no statistically significant reduction in meiotic pairing in either of our mutants. These results indicate that AKIR-1 is not required for either the establishment or the maintenance of pairing interactions and that the synapsis observed is homologous (unlike what was found in *htp-1* or

	Diakinesis –1			Diakinesis –3		
	Average (μm)	Fold over wild type	*n*	Average (μm)	Fold over wild type	*n*
Wild type	0.19	—	60	0.23	—	60
akir-1(RNAi)	0.3	1.6	60	0.29	1.3	60
akir-1(RNAi), spo-11	0.8	4.2	60	0.42	1.8	60
syp-2	1.37	7.2	90	1.1	4.8	84
spo-11	1.18	6.2	114	0.8	3.5	102
syp-2, spo-11	1.13	5.9	72	0.77	3.3	72
syp-2, akir-1	1.26	6.6	84	0.86	3.7	84
akir-1(RNAi), syp-2, spo-11	1.12	5.9	72	0.66	2.9	72

All pairwise comparisons between wild type, *akir-1*, and *akir-1; spo-11* and all other mutants is statistically significant (Mann–Whitney test; see Supplemental Table S2 for *p* values). *n* is the number of distances measured (*Materials and Methods*).

TABLE 1: Distance between DAPI-staining bodies measured at diakinesis –1 and –3.

htp-2 mutants; Couteau and Zetka, 2005; Martinez-Perez and Villeneuve, 2005).

SC disassembly is coordinated with crossover formation in wild-type nuclei (Nabeshima *et al.*, 2005). Thus defects in SC disassembly could be secondary to perturbations of crossover formation. In addition, a subset of mutants that affect asymmetric disassembly (*lab-1* and *htp-1/2*) affect crossover formation as well (de Carvalho *et al.*, 2008; Martinez-Perez *et al.*, 2008). We thus performed experiments to examine the possibility that the defects observed in *akir-1* mutants were secondary to defects in crossover formation.

RAD-51 is a strand-exchange protein required for DSB repair, acting downstream of DSB formation (Alpi *et al.*, 2003). RAD-51 forms foci on meiotic prophase I chromosomes (Colaiacovo *et al.*, 2003), which are a good indicator of the levels of DSBs in the *C. elegans* germline (Mets and Meyer, 2009). Increases in the levels of RAD-51 foci frequently correlate with defects in repair of DSBs through homologous recombination (MacQueen *et al.*, 2002; Colaiacovo *et al.*, 2003; Carlton *et al.*, 2006; Smolikov *et al.*, 2007, 2008, 2009). We counted the RAD-51 foci per nucleus in the gonads of *akir-1* mutants compared with wild type and found no significant increase at the regions where DSB repair occurs (zones 5–7, Figure 3, A–E, and Supplemental Table S3). Moreover, as in wild type, RAD-51 foci are not found in diplotene and diakinesis. Zones 4 and 5 show a slight decrease in RAD-51 foci; however the level of DSBs is high enough to support proper crossover formation (see later discussion). Apoptosis levels are somewhat elevated in *akir-1* mutants compared with wild type (wild type, 3.72, $n = 109$; *akir-1(gk528)*, 4.98, $n = 135$; $p = 0.002$, Mann–Whitney test). However, this increase is much lower than those observed in synapsis-defective mutants (3.5-fold increase for *syp-2(ok307)* to 13.15, $n = 71$, Mann–Whitney test). Therefore, it is likely that DSB repair is proficient in *akir-1* mutants.

In *akir-1* mutants, chromosomes still form bivalent-like, albeit highly abnormal, structures at diakinesis, as the number of DAPI-stained bodies observed in diakinesis is indistinguishable from wild type (wild type, 5.9 ± 0.3; *akir-1(rj1)*, 5.8 ± 0.5; *akir-1(gk528)*, 5.9 ± 0.3; $n = 41$, 45, 38 nuclei, $p = 0.52$, $p = 0.61$, Mann–Whitney test). Nevertheless, the pattern of SC disassembly can be influenced by the number of crossovers (Martinez-Perez *et al.*, 2008), and diakinesis bivalents are not always an indication of a mature crossover (Saito *et al.*, 2009). Therefore, we examined whether the number of crossovers is altered in *akir-1* mutants. We tested this by two methods: the cytological analysis of ZHP-3, a protein that localizes to the sites of crossovers (sex per nucleus; Bhalla *et al.*, 2008); and the direct examination of crossover frequencies using SNPs. We observed no difference in the number of ZHP-3 foci in *akir-1* mutants compared with wild type (Figure 3, F and G; *akir-1(rj1)/+*, 5.9 ± 0.7; *akir-1(rj1)*, 5.6 ± 0.8; $n = 37$, 60 nuclei, $p = 0.12$, Mann–Whitney test). Moreover, *akir-1(gk528)* mutants show no change in crossover frequencies (Table 2) compared with wild type. These data indicate that as in wild type, homologues are being held by crossovers in *akir-1* mutants. Taken together, our analysis shows that AKIR-1 acts downstream from crossover formation and is likely not involved in early aspects of prophase I chromosome dynamics.

akir-1 is required for proper diakinesis bivalent structure independent of condensin

A major event taking place in late prophase I is chromosome condensation. Chromosome morphology in *akir-1* mutants resembles that of wild type until diakinesis (Supplemental Figures S2A and S3; DAPI). As nuclei enter diakinesis, their bivalents exhibit two structural defects: 1) atypical diakinesis bivalent shape (Figures 1, D–G, inset, and 4, A and B) and 2) elongated chromosome arms (Table 3 and Figure 4, A and B).

In *C. elegans*, bivalent remodeling around a single crossover results in a cruciform structure with a small gap in the interface between the arms (Figure 4A, top). In *akir-1* mutants, diakinesis bivalents acquired an atypical shape (Figure 4A, bottom), including defects in the size of the gap region (Figure 4B). Half of the diakinesis bivalents of *akir-1* mutants acquired an aberrant cruciform shape (Figure 4A; $p < 0.0013$, Fisher's exact test, compared with wild type). This included an atypical arm positioning with detached axes for both homologues, a morphology that was never observed for wild-type diakinesis bivalents. In many cases this resulted in very little interface shared between each of the chromosome pairs, with only a thin chromatin thread connecting the two homologues. Moreover, diakinesis bivalents with wild-type cruciform structure frequently exhibited an enlarged gap region, almost twice as long in these mutants compared with wild type (Figure 4B, right). Because these structural defects are present in the region occupied by the SYP-1 aggregate, this suggests that SYP-1 aggregation may be a cause for this aspect of the diakinesis bivalent structural defect. To test this

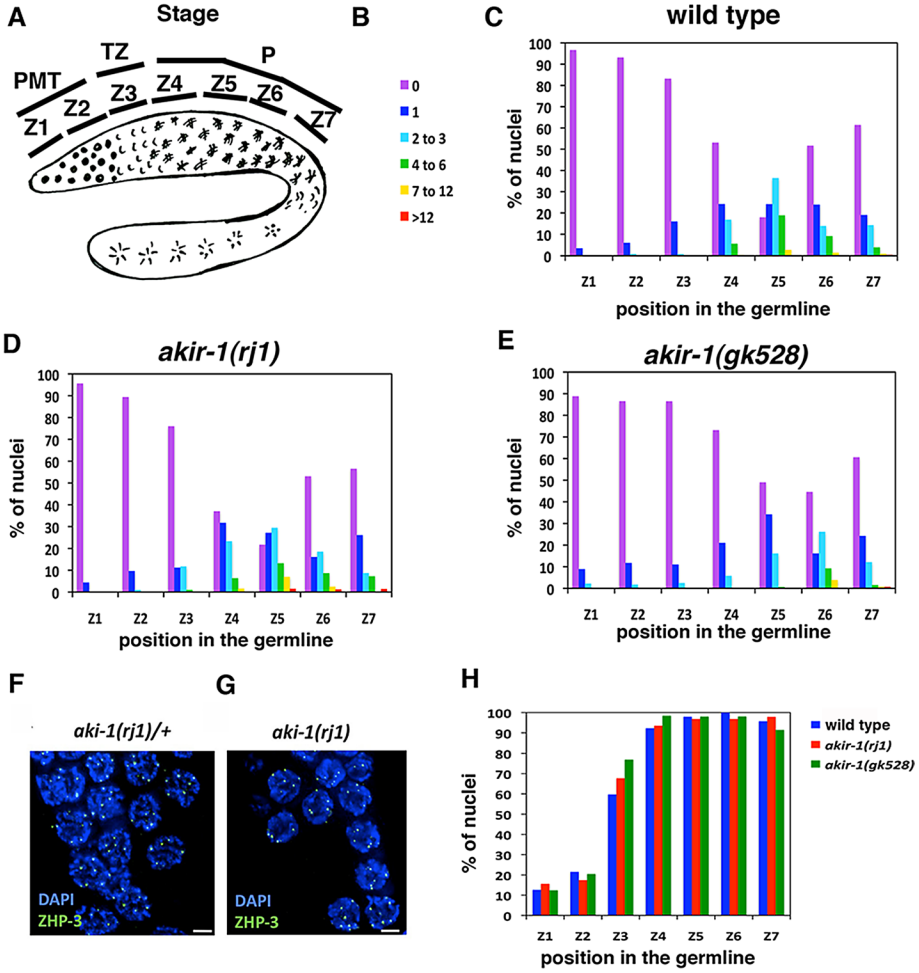

FIGURE 3: AKIR-1 is dispensable for meiotic pairing and recombination. Pairing initiation or stabilization, as well as recombination and crossover formation, is not affected in *akir-1* mutants. (A) Schematic representation of the gonad, representing the zone in the *x*-axis of C–E and H. Stages: PMT, premeiotic tip (mitotic division); TZ, transition zone; P, pachytene. (B) Color code for the graphs presented in C–E. (C–E) Quantitative analysis of the number of RAD-51 foci observed per nucleus in each gonadal zone examined. The *y*-axis indicates the percentage of nuclei in each range in each zone. (F, G) High-magnification images of nuclei of gonads from age-matched *akir-1(rj1)/+*, wild type for the phenotype examined (F), and *akir-1(rj1)* (G) mutants at late pachytene. (H) Quantitative analysis of pairing kinetics of wild type (blue), *akir-1(rj1)* mutants (red), and *akir-1(gk528)* mutants (green) at the 5S loci. The *y*-axis indicates the percentage of paired nuclei in each zone. Images are full projections through several nuclei stained with DAPI (blue) and containing GFP::ZHP-3 fusion protein (green). Bars, 2 μm.

hypothesis, we partially depleted the SYP complex by RNAi for *syp-2* in the *akir-1(gk528)* background. Under these conditions, bivalents are still formed; however, SYP aggregate formation is reduced. The reduction in aggregate formation was accompanied by a reduction in the size of the gap region (Figure 4B, right; $p << 0.001$, Mann–Whitney test), indicating that these changes in bivalent structure are caused by SYP aggregation.

The second structural defect observed was an increase in diakinesis bivalent size; the arms of each diakinesis bivalent were about twice as long compared with wild type (Table 3; $p < 0.001$ for both mutants, Mann–Whitney test). We wanted to ascertain whether these defects are simply the outcome of earlier SC disassembly defects or are independent of SC function. We examined chromosome length in *syp-1(me17)* mutants in the presence or absence of AKIR-1. Although *syp-1(me17)* mutants do not recruit any of the central region proteins to chromosomes, loading of axis and SC-associated proteins is not affected (MacQueen *et al.*, 2002; Colaiacovo *et al.*, 2003; Smolikov *et al.*, 2007, 2009). This allowed us to examine whether the requirement for AKIR-1 in maintaining chromosome structure is dependent on the central region proteins. Loss of SYP-1 protein results in the lack of crossover formation, leading to 12 univalents (Figure 4E; 11.8 ± 1, $n = 10$ diakinesis –1 oocytes; MacQueen *et al.*, 2002), but results in no significant change in chromosome length compared with wild type (Table 3 and Figure 4, C and E). SYP-1 is required for crossover formation and SC assembly regardless of AKIR-1, as *akir-1(gk528); syp-1(me17)* exhibits 12 univalents at diakinesis (11.8 ± 0.7, $n = 16$ diakinesis –1 oocytes) and a lack of functional SC (Supplemental Figure S6). However, the length of each univalent (Table 3) is increased in the double mutant; *akir-1(gk528)* deletion in the *syp-1* genetic background resulted in a 2.4-fold extension in the length of the chromosomes as compared with wild type (half diakinesis bivalent, one long arm and one short arm) or *syp-1* (univalent) (Table 3 and Figure 4, C–F; diakinesis –1, Mann–Whitney test, both $p < .001$). This result indicates that AKIR-1 is required for one aspect of chromosome structure—the length of the diakinesis bivalent—independent of the SC.

Condensation at the transition from diplotene to diakinesis is regulated by the condensin II complex and is independent of condensin I or condensin I^{DC}. Condensin-null mutants do not exhibit SC disassembly defects, indicating that condensation is not required for SC disassembly (Chan *et al.*, 2004; Supplemental Figure S7, E and F). To examine whether AKIR-1 acts in the condensin pathway, we first immunostained for MIX-1, a protein participating in all condensin complexes, in *akir-1(gk528)* mutants and observed no change in localization compared with wild type (Supplemental Figure S7, A–D). To test whether condensin II genetically interacts with *akir-1*, we depleted *akir-1* in mutants for two condensin II subunits, *capg-2(tm1833)* and *hcp-6(mr17)*. Because the effect on chromosome condensation in condensin II null mutants is already extremely severe (no bivalent structure), we cannot measure chromosome length in the double mutants of *akir-1*

	Nonrecombinant chromosomes	Recombinant chromosomes	Map distance (cM)
Wild type	133	61	31.4
akir-1(gk528)	114	50	30.5

Snip-SNP analysis revealed no significant change in crossover frequencies on chromosome II in *akir-1* mutants compared with wild type (Fisher's exact test, $p = 0.42$). SNPs used were pkP2101 and uCE2-2131.

TABLE 2: Crossover frequencies are not altered in *akir-1* mutants.

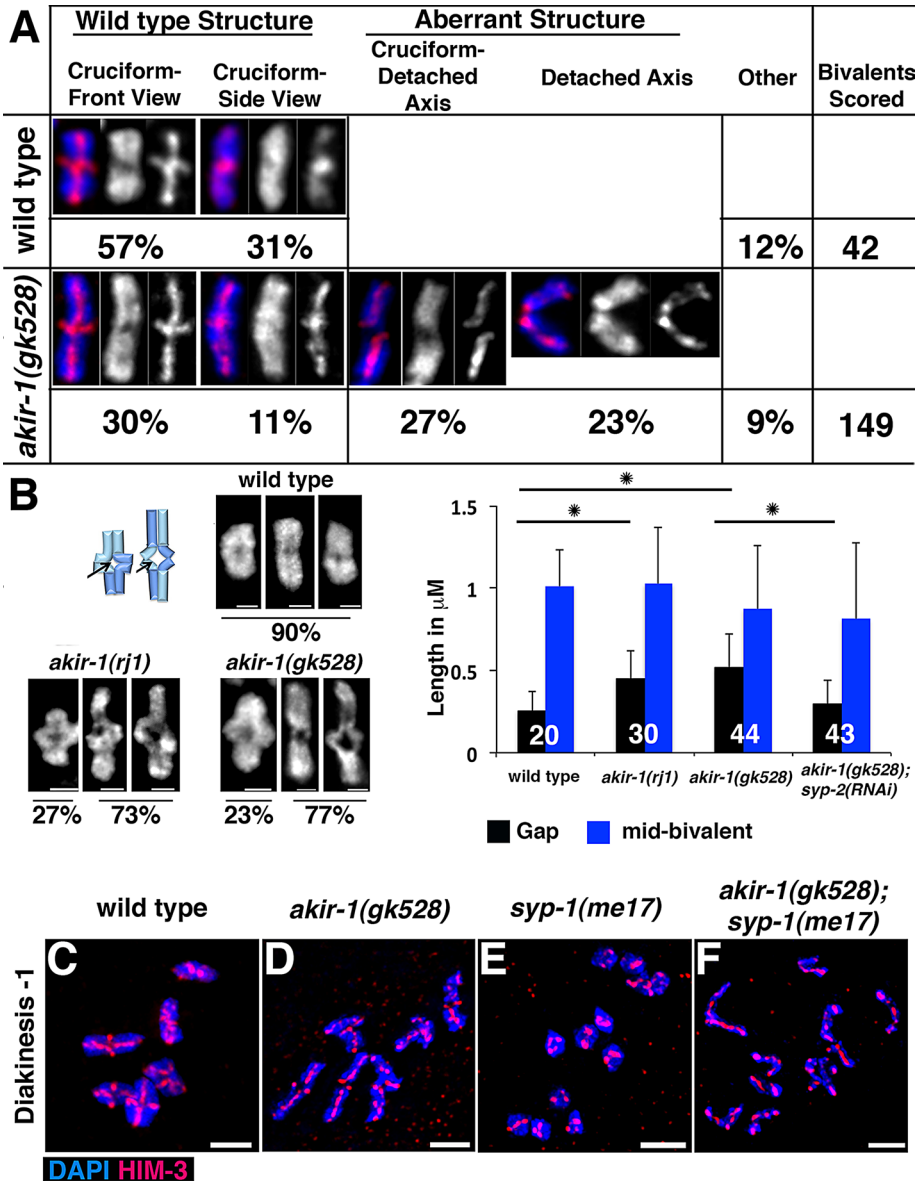

FIGURE 4: In *akir-1* mutants, chromosome structure is affected. *akir-1* mutants exhibit altered chromosome structure; 50% of bivalents lack the typical cruciform structure (A), increase in the size of the gap between the chromosomal arms (B), and increase in diakinesis bivalent length. (A) Chromosomes were stained with axial marker (HIM-3) and imaged at diakinesis –1. All three channels are shown on the left, DAPI only in the middle, and the antibody-only channel on the right. "Other" represents bivalents that do not belong to any of the categories indicated that were hard to score due to their positioning in the nucleus. (B, left) Schematic representation of a diakinesis bivalent, with wild type expected configuration on the left and mutant on the right. The gap is indicated with an arrow, and only forward-facing diakinesis bivalents were analyzed. The left image for *akir-1* mutants in B represents the minority of diakinesis bivalents that show wild-type configuration, whereas the two other images represent the majority of diakinesis bivalents, which are longer and contain a larger gap. (B, right) Chromosome length measured at diakinesis –1. Length of the region between homologous chromosomes is in blue, the length of the gap is in black. All gap-length comparisons between *akir-1* single mutants and wild type or *akir-1*; *syp-2(RNAi)* are highly statistically significant from each other (Mann–Whitney test, $p < 0.001$) and are indicated with asterisks. Differences between the *akir-1* single mutants are insignificant (Mann–Whitney test, $p > 0.05$). The *n* values are indicated on the graph. Error bars are SDs. (C–F) The increase in the length of the chromosomes in *akir-1* mutants is independent of SC. High-magnification images of diakinesis bivalents (A, B) or nuclei (C–F) of gonads from age-matched adult hermaphrodites of wild type (A, top; B, top; C), *akir-1(rj1)* mutants (B, left bottom) *akir-1(gk528)* mutants (A, bottom; B, right bottom, D), *syp-1(me17)* (E), and *akir-1(gk528); syp-1(me17)* (F) at diakinesis –3 (A) or diakinesis –1 (B–F). Gonads were stained with DAPI (blue) and HIM-3 (red, A, C–F). Bars, 1 μm (B), 2 μm (C–F).

with null condensin II mutants. Thus, to examine this question, we depleted *akir-1* by RNAi in *hcp-6(mr17)* at the semirestrictive temperature. Under these conditions, each of the single mutants showed an increase in chromosome length compared with wild type (Table 4 and Figure 5), whereas the double mutant showed an additive effect, supporting a model in which AKIR-1 acts in a separate pathway that affects chromosome structure. Moreover, no SC disassembly defects were observed in the *hcp-6(mr17)* mutant or were aggravated in the double mutants, indicating that AKIR-1's effect on SC disassembly is condensin independent. Like condensin II, condensin I/I^{DC} has no role in SC disassembly. Specifically, a condensin I/I^{DC} mutation had no effect on chromosome structure in late prophase, either as a single mutant or when combined with *akir-1(RNAi)* (the mutant examined is a null; Figure 5, I–P, and Table 4). Therefore, AKIR-1 regulates chromosome structure in the specific stage in which diakinesis bivalents are formed in an SC-dependent (cruciform formation) and SC-independent (chromosome length) manner and independently of condensin.

akir-1 mutants are largely proficient at AIR-2 and P-H3 recruitment, as well as at mitogen-activated protein kinase activation

The last events in meiotic prophase I involve oocyte maturation, the transition from diakinesis and metaphase of meiosis I. Oocyte maturation is supported by the activation of mitogen-activated protein kinase (MAPK) via its dephosphorylation (Miller *et al.*, 2001). Concurrently, in diakinesis –1 oocytes, AIR-2 is recruited to chromosomes (Schumacher *et al.*, 1998; Rogers *et al.*, 2002) to mediate histone H3 phosphorylation (P-H3; Hsu *et al.*, 2000) on the sister chromatids of the short arm of the bivalent, the site of cohesion removal at MI (mid–bivalent region; Nabeshima *et al.*, 2005; de Carvalho *et al.*, 2008). We examined whether these events occur properly in *akir-1* mutants.

In *akir-1* mutants, AIR-2 and P-H3 localized to the mid–bivalent region, as observed in wild type (Figure 6, A–J). However, in contrast to wild-type nuclei (Figure 6, D and G), P-H3 failed to colocalize with the chromosome-associated SYP-1 in *akir-1* mutants (Figure 6, E, F, and H–J). In these chromosomes, P-H3 was positioned in close proximity to the chromosomal arms, whereas SYP-1 was found further away from them (Figure 6J). The activated form of MAPK was found in the large majority of diakinesis –1 oocytes from wild type (93% of diakinesis –1

	Diakinesis –3: length (μm) of a diakinesis bivalent (*n*)	Diakinesis –1		
		Length (μm) of a diakinesis bivalent (*n*)	Length (μm) of one homologue (*n*)	Fold change over wild type
Wild type	2.1 (43)	2.1 (42)	1.1 (42)	—
akir-1(rj1)	4.9 (54)	3.7 (30)	1.8 (30)	1.5*
akir-1(gk528)	4.6 (54)	3.3 (84)	1.7 (84)	1.5*
syp-1	NA	NA	1.2 (54)	1.1
akir-1(gk528); syp-1	NA	NA	2.6 (48)	2.4*

Length of a diakinesis bivalent is an accumulative length of both arms (for details of measurement see *Materials and Methods*). *syp-1* mutants lack crossover events, and therefore diakinesis bivalents are not formed (NA), and single chromosomes were measured. For comparison to he length of the other genetic backgrounds, diakinesis bivalent length is divided by 2 as well (one short and one long arm). All values are highly statistically significant from each other (asterisk; Mann–Whitney test, $p < 0.001$), except wild-type diakinesis –3 to –1, diakinesis –1 *akir-1(gk528)* to *akir-1(rj1)*, and diakinesis –1 wild type to *syp-1*, which are not statistically significant ($p = 0.74$, 0.94, 0.5, respectively) and diakinesis –1 *akir-1(gk528)* to *akir-1(rj1)*, which is marginally significant ($p = 0.02$).

TABLE 3: Chromosome length measured at diakinesis –1 and diakinesis –3.

oocytes, $n = 60$; Figure 6K) as well as *akir-1* mutants (72% of diakinesis –1 oocytes, $n = 97$; Figure 6L), indicating proficient oocyte activation. All mutant diakinesis –1 oocytes contained SYP aggregates and condensation-impaired bivalents. Therefore, SC disassembly and condensation defects are not caused by the inability to activate oocytes in *akir-1* mutants. Of interest, whereas no diakinesis –1 oocytes in wild-type worms lacked P-H3 staining ($n = 53$), a significant fraction of *akir-1* mutant oocytes had no P-H3 staining (diakinesis –1 oocytes: *akir-1(rj1)*, 25%; *akir-1(gk528)*, 10%; $n = 57$, 58 oocytes; $p < 0.001$, $p = 0.028$, Fisher's exact test). These numbers are similar to the percentage of oocytes that do not show MAPK activation in *akir-1* mutants.

AKIR-1 is required for proper meiotic divisions

akir-1 mutants exhibit increased embryonic lethality, which could be due to errors in the meiotic divisions or to postmeiotic events. Such errors could include defects in the formation of the meiotic spindle. To test this, we performed live imaging, as well as examined fixed samples, of *akir-1(rj1)* mutants containing histone H2B fused to mCherry (to visualize chromosomes) and α-tubulin fused to GFP (TBA-2, to visualize the spindle; Wignall and Villeneuve, 2009). *akir-1(rj1)* mutants formed a distinctive meiotic spindle (Figure 7, B and D; normal spindle: MI, 98%; MII, 100%; $n = 46$, 44 fertilized oocytes) with no apparent deviations ($p = 1$, Fisher's exact test) from the wild-type spindle structure (Figure 7, A and C; normal spindle: MI, 99%; MII, 98%; $n = 69$, 43 fertilized oocytes). Embryonic lethality may result from defects in the segregation of chromosomes at either one, or both, of the meiotic divisions. As expected, no segregation defects were observed in wild-type fertilized oocytes during both meiotic divisions (Figure 7, E and G; *n* fertilized oocytes at MI, MII = 28, 21). However, *akir-1* mutants exhibited a high frequency of aberrant chromosomal segregation patterns at MI (Figure 7, F and F′, and Supplemental Table S4; *akir-1(rj1)*, 23%, $n = 28$, 31 MI fertilized oocytes, wild type vs. mutants, $p = 0.001$, Fisher's exact test) and MII (Figure 7, H and H′, and Supplemental Table S4; *akir-1(rj1)*, 33%, $n = 21$, 24 MII fertilized oocytes, wild type vs. mutants, $p = 0.004$, Fisher's exact test). These defects included lagging chromosomes, misaligned chromosomes, and, to a much lesser extent, condensation defects. No chromosome bridges were observed. Because both divisions are similarly impaired in *akir-1* mutants, this could be attributed to defects in sister chromatid cohesion. However, defects in loading the cohesin complex are probably not the cause for these phenotypes, since immunostaining for REC-8, one of the meiotic-specific cohesin proteins (Pasierbek *et al.*, 2001; Severson *et al.*, 2009), localized to gonadal nuclei in *akir-1* mutants indistinguishably from wild-type nuclei (Supplemental Figure S8).

The aberrant chromosomal segregation patterns may explain the ~20% of embryonic lethality and the very weak Him phenotype (indicative of X chromosome nondisjunction) in the *akir-1* mutants. However, measurements of chromosome nondisjunction (Supplemental Table S5) indicate that surviving embryos do not show high levels of nondisjunction (this assay cannot exclude low levels and/or few chromosomes involved in nondisjunction). It is possible that the lagging and misaligned chromosomes observed do not result in

	Diakinesis –1: length (μm) of a diakinesis bivalent (*n*)	Diakinesis –3: length (μm) of a diakinesis bivalent (*n*)	Fold over wild type (diakinesis –1, diakinesis –3)
Wild type	2.7 (48)	3.18 (48)	NA
akir-1(RNAi)	4.08 (48)	4.45 (48)	1.5, 1.4
hcp-6(mr17)	3.11 (48)	3.81 (48)	1.2, 1.2
akir-1(RNAi); hcp-6(mr17)	4.49 (48)	6.31 (48)	1.6, 2.0
dpy-28(s939)	2.81 (42)	3.27(42)	1.0, 1.0
akir-1(RNAi); dpy-28(s939)	3.93 (54)	4.91 (48)	1.4, 1.5

Length of a diakinesis bivalent is an accumulative length of both arms (for details of measurement see *Materials and Methods*). All values are statistically significant from each other (Mann–Whitney test $p < 0.001$), with the following exceptions: wild type to *dpy-28(s939)* and *akir-1(RNAi)* to *akir-1(RNAi); dpy-28(s939)*, which are not significantly different.

TABLE 4: Chromosome length measured at diakinesis –1 and diakinesis –3.

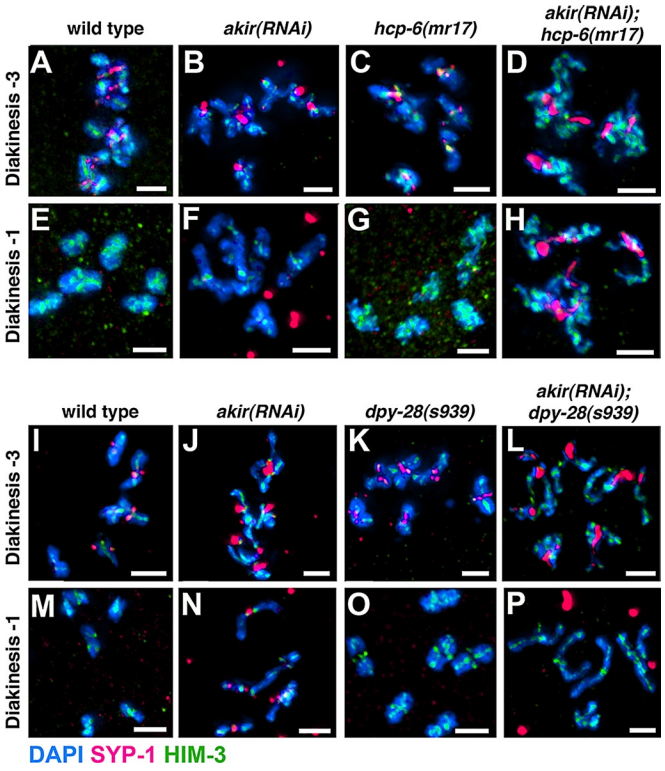

FIGURE 5: AKIR-1 affects meiotic chromosome structure independently of condensin. *akir-1* mutants exhibit altered diakinesis bivalent structure, a phenotype that is additive with condensin II mutants (A–H) but not with condensin I/I^{DC} mutants (I–P). SYP-1 aggregates are formed and fail to disassemble at the end of meiotic prophase I in *akir-1* mutants but not in condensin mutants. High-magnification images of stained nuclei in gonads from age-matched wild type (A, E, I, M), *akir-1(RNAi)* mutants (B, F, J, N), condensin II mutants *hcp-6* (C, G), and condensin I/I^{DC} mutants *dpy-28* (K, O), *akir-1(RNAi); hcp-6* (D, H) and *akir-1(RNAi); dpy-28* (L, P). Diakinesis –3 (A–D, I–L), diakinesis –1 (E–H, M–P). Nuclei are stained with DAPI (blue) and SYP-1 (red) and HIM-3 (green). Images are full projections of a single nucleus. Bars, 2 μm.

embryos with nondisjunction since they are repaired before the completion of each meiotic division. If this is so, meiotic lagging/misaligned chromosomes will either halt or delay the meiotic divisions, which allows the repair of their misalignment. To test this, we analyzed the timing of both meiotic divisions using live imaging. Our findings indicate that both MI and MII are about twice as long in *akir-1(rj1)* as in wild type (Table 5 and Supplemental Movies 1–10). These data are consistent with a model in which lagging chromosomes delay the meiotic divisions in *akir-1* mutants to allow chromosomes to realign and properly segregate. Our model is presented in Supplemental Figure S9.

DISCUSSION

Acquiring proper diakinesis bivalent structure is a prerequisite for accurate chromosome segregation in meiosis, as shown by many studies demonstrating that altered chromosome condensation perturbs progression through meiosis. Our findings now provide an additional mechanism for maintaining proper bivalent structure: through analysis of a novel meiotic gene, *akir-1*, we demonstrate a role for SC disassembly in restructuring the diakinesis bivalent. Our studies identify a previously unknown meiotic role for the conserved metazoan *akirin* gene family, specifically for *akir-1* in *C. elegans*. *akir-1* is the first gene identified to play a role in the resolution of the short chromosome arm and is an important new component of the mechanisms regulating SC disassembly and chromosome condensation.

AKIR-1 is essential for proper diakinesis bivalent structure in late prophase

In *C. elegans*, condensin II–dependent bivalent condensation acts at the diplotene-to-diakinesis transition, concurrent with but independent of SC disassembly (MacQueen *et al.*, 2002; Colaiacovo *et al.*, 2003; Chan *et al.*, 2004; Smolikov *et al.*, 2007, 2009). Our data show that AKIR-1 acts in a distinct pathway from that of condensin to modulate chromosome structure in meiosis. The condensation defects observed in *akir-1* mutants are, however, milder than those observed for condensin II null mutants, in which diakinesis bivalent structure cannot even be detected. In addition, since most *akir-1* mutant chromosomes eventually condense at the exit from prophase I, AKIR-1's role in condensation seems to be restricted to late meiotic prophase I. The identification of this distinct pathway involving AKIR-1 adds a new layer of regulation to chromosome behavior at this important meiotic stage.

AKIR-1 regulates short-arm resolution through its role in central region disassembly

Proteins involved in SC disassembly have been identified in numerous model organisms (Ivanovska *et al.*, 2005; Malmanche *et al.*, 2007; Bhalla *et al.*, 2008; de Carvalho *et al.*, 2008; Martinez-Perez *et al.*, 2008; Sourirajan and Lichten, 2008; Jordan *et al.*, 2009, 2012; Peretz *et al.*, 2009; Resnick *et al.*, 2009). Unfortunately, mutations in these genes lead to multiple meiotic defects in addition to disrupting SC disassembly. Thus it is possible that that the role of these proteins in SC disassembly is indirect. Alternatively, it may be a reflection of a biological program in which pathways controlling other key aspects of meiosis are coopted to regulate SC disassembly. AKIR-1 seems to fit this latter model, being a protein with multiple roles in meiosis.

The disassembly of SC proteins in *C. elegans* occurs through distinct mechanisms in the short versus the long arm of the bivalent. AKIR-1 is the only known player in the process of short-arm resolution, which is mechanistically distinct from the asymmetric disassembly processes occurring on both arms. We propose a role for AKIR-1 in preventing the accumulation of SYP proteins on chromosomes once SC disassembly is initiated and SYPs are removed from the long arm of the diakinesis bivalents. Our data agree with a model in which AKIR-1 prevents SYPs that have unloaded from the long arms of the chromosomes from reassociating with SYPs still bound to the short arms. This process is crucial for disabling the SYPs from connecting homologues while they are still associated with chromosomes in diakinesis. In *akir-1* mutants, SYPs bind and form aggregates on the short arm of the diakinesis bivalent, delaying arm resolution. We propose that this accumulation of SYPs pushes the chromatin in different directions, expanding the gap in the interface between the arms and distorting the structure of the bivalent. When central region proteins are removed from chromosomes before fertilization, the region normally bound by the SYPs appears as a widened gap, resulting in aberrant diakinesis bivalent structure, which may account for the meiotic division defects observed in the mutants.

The interplay between central region disassembly and diakinesis bivalent structure

Our results point to an interplay between chromosome restructuring and SC disassembly, two key events in late prophase I. We suggest that AKIR-1 modulates chromosome structure in late meiotic prophase I by 1) regulating chromosome condensation (length) in an

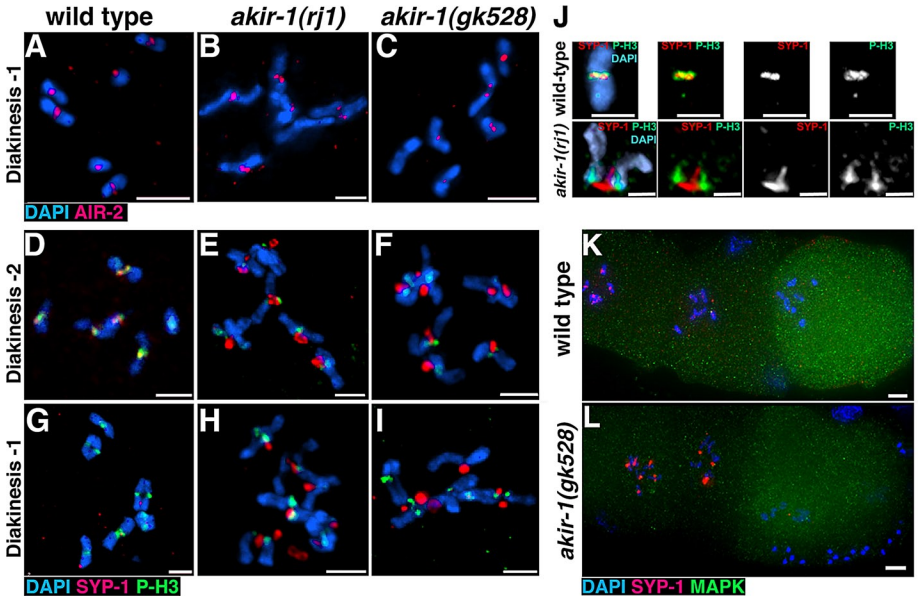

FIGURE 6: *akir-1* mutants are largely proficient at AIR-2 and P-H3 recruitment and at MAPK activation. (A–I) *akir-1* mutation does not prevent the localization of proteins involved in sister chromatid cohesion removal to the short-arm region. (J) Wild-type bivalents exhibited colocalization of SYP-1 and P-H3 at the mid–bivalent region. This colocalization is absent in the *akir-1(rj1)* bivalent, when the SYP-1 aggregate is positioned between the two homologues, whereas P-H3 is present on chromosomes at what is equivalent to the short-arm region. (K–L) MAPK is activated in the majority of *akir-1* oocytes. *akir-1* mutants are stinted with phosphorylated MAPK. High-magnification images from age-matched wild type (A, D, G, J, K), *akir-1(rj1)* mutants (B, E, H, J), *akir-1(gk528)* mutants (C, F, I, L), and adult hermaphrodites at diakinesis –2 (D–F, J) or diakinesis –1 (A–C, G–I). All gonads were stained with DAPI (blue) and SYP-1 (red, D–L) or AIR-2 (red, A–C), as well as P-H3 (green, D–J) or activated MAPK (green, K–L). Images show an overlay of channels, except in J, for P-H3 and SYP-1 (middle left), SYP-1 only (middle right), and P-H3 only (right). Images are full projections of a single nucleus (A–I), a bivalent (J), or last three oocytes (K–L). Bars, 1 μm (J), 2 μm (A–I), 5 μm (K–L).

SC- and condensin-independent manner and 2) supporting cruciform shape by promoting proper short-arm resolution in an SC-dependent manner. The current view is that condensation is not required for SC disassembly in *C. elegans* (Chan *et al.*, 2004). Therefore it is likely that the two functions of AKIR-1 in chromosome structure are independent of each other. An alternative hypothesis is that AKIR-1 could affect condensation directly, which in turn affects SC disassembly indirectly. In this case, that would be the first demonstration of a protein affecting SC disassembly through its role in condensation in *C. elegans*. Regardless of the molecular role AKIR-1 plays in meiosis, our findings reveal an important role for AKIR-1 in meiotic chromosome behavior and forge a link between proper SC disassembly and acquiring a functional bivalent structure at diakinesis.

Meiotic prophase I progression and AKIR-1

Whereas meiotic divisions are delayed in *akir-1* mutants, meiotic prophase I progresses normally. The kinetics of meiotic events such as pairing, DSB formation and repair, loading of SC proteins, and clustering and dispersal of chromosomes are all unaffected in *akir-1* mutants. Moreover, staining for active MAPK indicates that *akir-1* mutant oocytes are activated and able to mature. The only alteration in meiotic prophase I progression is a reduced number of diakinesis nuclei in *akir-1* mutants. However, this is likely not causal to SC disassembly, as mutants with a more severe reduction in the numbers of diakinesis nuclei have no defects in SC disassembly. Moreover, if the phenotypes we observe were an outcome of general meiotic progression defects, it would be hard to explain why *akir-1* mutation affects specifically all four SYPs without affecting all other SC proteins.

AKIR-1 and transcription

AKIRIN encodes an evolutionarily conserved protein with a somatic role in transcription through its interaction with DNA-binding proteins, including chromatin remodelers and transcription factors (Goto *et al.*, 2008; Komiya *et al.*, 2008; Nowak *et al.*, 2012). This raises the possibility that AKIR-1's functions in meiosis might involve transcription as well. We believe it likely, however, that the meiotic and somatic mechanisms of action of AKIRIN proteins are distinct and that AKIR-1 does not act in transcription in the worm germline. Several results support this conclusion. First, in the *C. elegans* germline, protein expression is generally regulated translationally and not transcriptionally (Merritt *et al.*, 2008). Second, transcription is repressed at diakinesis, the stage in which *akir-1* mutants exhibit their strongest phenotype. Third, the level of SYP-1 transcript is no different in *akir-1* mutants and wild type. Finally, other studies have shown that proteins acting as transcription factors in somatic tissues adopt different roles in meiosis (e.g., HIM-8; Phillips *et al.*, 2005). The further investigation of the meiotic and somatic functions of *akirin* in both *C. elegans* and other model organisms will be required for a complete understanding of the complex biological roles played by this conserved protein family. The data we present here represent an important step forward, identifying the worm AKIR-1 orthologue and demonstrating a novel function for this protein in meiosis. This role, outside transcription, reflects the versatile functions of this conserved protein that may be relevant to its somatic functions as well.

MATERIALS AND METHODS

Strains

All *C. elegans* strains were cultured under standard conditions at 20°C (Brenner, 1974). Bristol N2 worms were use as the wild-type background, and Hawaiian CB4856 wild-type worms were used for SNP mapping in the process of cloning *akir-1(rj1)*. The following mutations and chromosome rearrangements were used (McKim *et al.*, 1993; Dernburg *et al.*, 1998; MacQueen *et al.*, 2002; this work):

LGI: akir-1(rj1), akir-1(gk528), hcp-6(mr17), hT2[bli-4(e937) qIs48] (I;III)

LGIII: dpy-28(s939)

LGIV: spo-11(ok79)

LGV: syp-1(me17), *syp-2*(ok307), *capg-2*(tm1833)

The following transgenic lines were used:

UV7 unc-119(ed3) III; jfIs2[pie-promoter::GFP::zhp-3 + unc-119(+)] (Bhalla *et al.*, 2008)

OD57 unc-119(ed3); ltIs37 [pAA64: pie-1p::mCHERRY::his-58 + unc-119 (+)]; ltIs25 [pAZ132; pie-1p::GFP::tba-2 + unc-119 (+)] (McNally *et al.*, 2006)

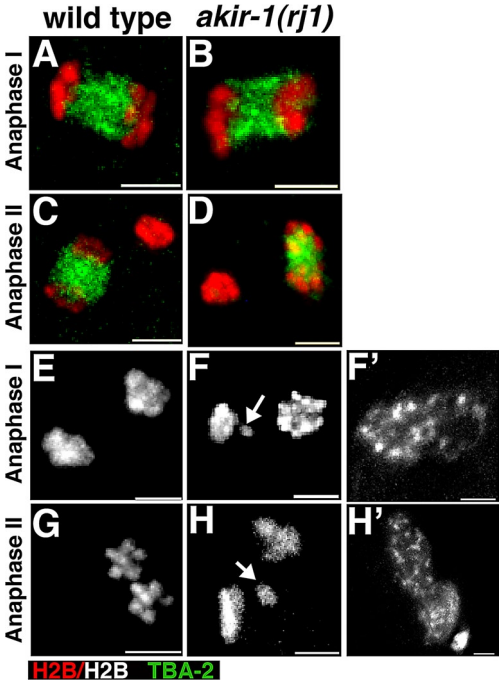

FIGURE 7: Chromosome segregation is perturbed in *akir-1* mutants undergoing meiosis I and II. Lagging (F, H) and decondensed (F′, H′) chromosomes were observed in both meiotic divisions in *akir-1(rj1)* mutants, whereas the spindle still formed as observed in wild type (A–D). Arrows point to lagging chromosomes. High-magnification images of chromosomes from fertilized oocytes of age-matched adult hermaphrodites of wild type (A, C, E, G) and *akir-1(rj1)* mutants (B, D, F, H) at anaphase I (A, B, E–F′) and II (C, D, G–H′). Chromosomes are visualized by *mCherry::H2B* (red, A–D; or white, E–H′) and *GFP::tba-2* (α-tubulin, green, A–D) fusion proteins. Images are full projections of all chromosomes. Bars, 2 μm.

Characterization and isolation of *akir-1* alleles

We isolated the *rj1* allele in a forward genetic screen using ethane methyl sulfonate as a mutagen. Because meiotic mutants will develop into healthy adults that produce many inviable eggs, we screened for mutants that exhibit a maternally rescued embryonic-lethal phenotype. We then performed a secondary, cytology-based screen to identify those mutants in which SC disassembly was specifically affected. This screen used high-resolution imaging techniques to identify mutants with aberrant SC localization at diakinesis via immunostaining for SYP-1. The mutation was linked to a SNP located at the −1-cM position on chromosome I. In addition, deficiency analysis pointed to *rj1* being located in the region encompassed by sDf4. Genome-wide sequencing indicated that four genes in this region contained nonsynonymous mutations, using methodology previously described (Rose *et al.*, 2010). The presence of the *rj1* mutation was verified by Sanger sequencing. These four genes were examined for prophase I cytological phenotypes of any existing allele and/or RNAi-mediated depletion for these ORFs (RNAi was performed as in Timmons *et al.* [2001], except that 1 mM isopropyl-β-D-thiogalactoside was used). Both the *gk528* allele and RNAi for E01A2.6 phenocopied the *rj1* phenotype. Neither RNAi or allele analyses to any of the other genes exhibited a meiotic prophase I phenotype. RNAi for *akir-1* was performed using pL4440, to which the entire predicted E01A2.6 cDNA was cloned. The *rj1* allele contains a histidine-to-proline substitution at position 190.

The *gk528* allele was generated by the *C. elegans* Reverse Genetics Core Facility at the University of British Columbia (Vancouver, Canada), which is part of the International *C. elegans* Gene Knockout Consortium. It contains a 678–base pair deletion including exon 1 and extending halfway into exon 2 of open reading frame E01A2.6. The deletion also removes most of the predicted promoter and 42% of the coding region. The *gk528* deletion is expected to remove a small ORF (E01A2.9) with unknown function nested in the first intron of the gene. Because *gk528* does not exhibit more severe phenotype compared with its RNAi or the *rj1* allele, E01A2.9 is likely not involved in meiosis or may not be a functional gene. *akir-1(gk528)* exhibits the same phenotype as *akir-1(rj1)* and *akir-1(rj1)/akir-1(gk528)* (Figure 1), supporting the argument that both strains contain alleles of the same gene. Moreover, the phenotype caused by *akir-1(RNAi)* was indistinguishable from the phenotype caused by the two *akir-1* alleles.

Both *rj1* and *gk528* are recessive *akir-1* alleles (DAPI- and SYP-1–stained germlines of *rj1*/+ and *gk528*/+ hermaphrodites were identical to wild-type germlines). We showed that these two alleles exhibit indistinguishable phenotypes based on all assays to be described. However, the penetrance of some of the phenotypes was significantly higher for the point-mutant allele (*rj1*) compared with the deletion allele (*gk528*). This includes embryonic lethality (21 vs. 16%, $p = 0.05$, Fisher's exact test, $n = 456, 755$), percentage of aggregates associated to chromosomes at diakinesis –1 (60 vs. 30%, $p < 0.001$, Fisher's exact test, $n = 108, 108$), reduction in P-H3 staining (25 vs. 10%, $p < 0.04$, Fisher's exact test, $n = 57, 58$), number of oocytes in diakinesis (3.3 vs. 4.6, $p < 0.001$, Mann–Whitney test, $n = 30, 24$). This may indicate that our point-mutant allele is not a complete loss of function but exhibits some recessive gain-of-function properties. However, this does not change our main conclusions, as the phenotypes are consistent and of similar degree between the two alleles. The present results suggest that *akir-1(gk528)* is a null and *akir-1(rj1)* is close to being a null. Both of the mutant phenotypes (SC disassembly and diakinesis bivalent structure defect) were evident in every oocyte and diakinesis bivalent examined in all mutant genotypes.

	MI		MII	
	Duration (min)	*n*	Duration (min)	*n*
Wild type	6.66	4	11.88	6
akir-1(rj1)	14.53	8	20.95	10
Mann–Whitney test: *p* value	0.007		0.017	

Differences between wild type and mutants are statistically significant. The duration of MI was measured from the departure from the spermatheca (ovulation) to the extrusion of the first polar body. The duration of MII was measured from the extrusion of the first polar body to the extrusion of the second polar body.

TABLE 5: Timing of meiotic divisions in wild type and *akir-1* mutants, based on live imaging.

Germ cell apoptosis

Germ cell corpses were scored in adult hermaphrodites 20 h post-L4 as in Kelly *et al.* (2000). Statistical comparisons between genotypes were performed using the two-tailed Mann–Whitney test, 95% confidence interval.

Crossover recombination frequencies

Meiotic crossover recombination frequencies were assayed using SNP markers as in Hillers and Villeneuve (2003). *akir-1* was introgressed into the Hawaiian strain CB4856 by six outcrosses. Because of the embryonic lethality observed for *akir-1(gk528)* mutants and

the unsuccessful mating of homozygote males, recombination frequencies were assayed on homozygotes generated by mating *akir-1(gk528)* hermaphrodites from the Hawaiian strain CB4856 background to *akir-1(gk528)/hT2*[*bli-4(e937)qIs48*] males from the Bristol (N2) background. The F2 generation of hermaphrodites that were homozygous for *akir-1(gk528)* and heterozygous for SNP markers were analyzed. The presence of homozygous alleles of *akir-1(gk528)* was verified by PCR. The SNPs used were pkP2101 and uCE2-2131 as in Davis *et al.* (2005).

Nondisjunction frequencies using restriction fragment length polymorphism assay

Meiotic nondisjunction frequencies were assayed using the restriction fragment length polymorphism (RFLP) assay developed by Severson *et al.* (2009). We modified this assay by using nested PCR to increase the reliability of the amplification. Primers used for primary PCR, GACGGAGAATGAGATTCTGCAGG and GCTCCGTGTGCTTTCTGTGACG. Primers used for secondary PCR, CGGCTCGTCTTATGAAACGGA and GTGAGCCCGTTAAAAATCCA.

Reverse transcription-PCR

To determine the relative levels of SYP-1 expression, reverse transcription (RT)-PCR was performed on mRNA extracted from whole worms in duplicates (RNEasy kit; Qiagen, Valencia, CA) and subjected to reverse transcription with SuperScript III Reverse Transcriptase (Invitrogen, Carlsbad, CA). For quantitative RT-PCR, SYBR Green I Master Kit was used (Roche, Indianapolis, IN) and read in Roche LightCycler480 Real-Time PCR System. For each mRNA extracted, three technical controls were made. For *syp-1* the following primers were used: gatgaaatgataattcgccaaga and acgcaatcttccctcatttg. For *myo-3* control the following primers were used: tccggatccagaagatgg and accacggtcacctgttcg.

FISH and time-course analysis of chromosome pairing

The 5S FISH probe was generated as in Dernburg *et al.* (1998) from a PCR fragment generated by amplifying *C. elegans* genomic DNA with the 5′-TACTTGGATCGGAGACGGCC-3′ and 5′-CTAACTGGACTCAACGTTGC-3′ primers. Fragments were labeled with fluorescein-12-dCTP (PerkinElmer, Waltham, MA). Homologous pairing was monitored quantitatively as in MacQueen and Villeneuve (2001). The average number of nuclei scored per zone (*n*) from three gonads each for wild type, *akir-1(rj1),* and *akir-1(gk528)* are as follows: zone 1, 95; zone 2, 109; zone 3, 115; zone 4, 106; zone 5, 97; zone 6, 96; and zone 7, 78). Pairing was similar or higher for any of the mutants compared with wild type in all meiotic zones except for zones 6 and 7, in which *akir-1(gk528)* was lower but not statistically significant ($p = 0.206$, $p = 0.371$, Fisher's exact test), and except for zones 5 and 6, in which *akir-1(rj1)* was lower but not statistically significant ($p = 0.678$, $p = 0.115$, Fisher's exact test). Therefore there is no statistically significant reduction in pairing in *akir-1* mutants.

Immunostaining and microscopy

Unless stated otherwise, images were collected from all bivalents in each oocyte imaged, to prevent any bias in image analysis. DAPI staining, immunostaining, and analysis of stained meiotic nuclei were performed as in Colaiacovo *et al.* (2003), except REC-8 staining (Rogers *et al.*, 2002), P-H3 and AIR-2 (Hsu *et al.*, 2000). Primary antibodies were used at the following dilutions: goat α-SYP-1, 1:500 (MacQueen *et al.*, 2002); rabbit α-SYP-2, 1:100 (Colaiacovo *et al.*, 2003); rabbit α-SYP-3, 1:100 (Smolikov *et al.*, 2007); rabbit α-RAD-51, 1:100 (Colaiacovo *et al.*, 2003); rabbit α-HIM-3, 1:500 (Zetka *et al.*, 1999); guinea pig α-HTP-3, 1:500 (Goodyer *et al.*, 2008); mouse α-REC-8, 1:50 (Abcam, Cambridge, MA); rabbit α-LAB-1,1:300 (de Carvalho *et al.*, 2008); rabbit α-P-H3, 1:400 (Millipore, Billerica, MA); diphosphorylated MAPK, 1:500 (Sigma-Aldrich); and rabbit α-MIX-1, 1:100. The secondary antibodies used were Alexa Fluor 555 anti-rabbit (Invitrogen), fluorescein isothiocyanate α-rabbit, Alexa Fluor 568 anti–guinea pig (Invitrogen), DyLight 594 anti-goat (Jackson Immunochemicals, West Grove, PA), and Cy3 α-mouse (Jackson Immunochemicals), each at 1:500.

For MI and MII analysis, *akir-1(rj1)* was introduced into the OD57 genetic background (*pie-1p::mCHERRY::his-58* and *pie-1p::GFP::tba-2*). Fertilized oocytes were assessed either by live imaging or after ethanol fixation. MI and MII data for *akir-1(gk528)* were collected for ethanol-fixed and DAPI-stained fertilized oocytes. Quantitative analysis of the intensity of SYP-1 signals was performed using softWoRx 5.0.0 software (Applied Precision, Issaquah, WA). This was performed under guided model option with a freehand polygon section in all *Z*-stacks of a particular SYP signal and to multiple gonads from each genetic background. To obtain SYP-1 signal intensity, we subtracted the background of the same image from the SYP-1 signal intensity read.

For time-lapse differential interference contrast (DIC) microscopy, control (*pie-1p::mCHERRY::his-58* and *pie- 1p::GFP::tba-2*) and *akir-1(rj1) pie-1p::mCHERRY::his-58* and *pie-1p::GFP::tba-2* worms were anesthetized in 0.1% tricaine/0.01% tetramisole in M9 and immediately mounted on 2% agarose pads with 8 µl of the anesthetic and covered with a 22-mm square glass coverslip. Tricaine/tetramisole paralyzes body wall movement but does not block several rounds of oocyte maturation and ovulation. Images were captured at room temperature using DIC microscopy and recorded every 3–4 s for up to 44 min using SoftWoRx 5.0.0 software. Movies were compiled at 10–13 frames/s. No photodamage was observed during the course of the experiment.

The images were acquired using the DeltaVision wide-field fluorescence microscope system (Applied Precision) with Olympus 100×/1.40 lenses (except for S3, with 60× lenses). Optical sections were collected at 0.20-µm increments with a CoolSNAP$_{HQ}$ camera (Photometrics, Tucson, AZ) and softWoRx software and deconvolved using softWoRx 5.0.0 software. Pachytene images are projections halfway through three-dimensional data stacks of whole nuclei (15–30 0.2-µm slices/stack), and diakinesis images encompass entire nuclei; both were prepared using softWoRx 5.0.0 and softWoRx Explorer 1.3.0 software (Applied Precision).

Time-course analysis for RAD-51 foci

Quantification of RAD-51 foci was performed for all seven zones composing the premeiotic tip to late pachytene regions of the germline as in Colaiacovo *et al.* (2003). The total number of nuclei scored per zone from three gonads each for wild type, *akir-1(rj1),* and *akir-1(gk528)* are as follows: zone 1, 242; zone 2, 263; zone 3, 213; zone 4, 217; zone 5, 170; zone 6, 169; and zone 7, 137. Statistical comparisons between genotypes were performed using the two-tailed Mann–Whitney test, 95% confidence interval.

Analysis of chromosomal features and distances

Because *akir-1* mutants have diakinesis bivalent structure defects (see later discussion), in chromosomes lacking the typical cruciform structure we defined the long arm of the diakinesis bivalent as the longer portion of the chromosome up to the region where the two chromosomes connect and the shorter arm as the remaining portion of each chromosome. Because *akir-1* mutant chromosomes are longer than wild type but are confined to the same nuclear space, resolving individual chromosomes was challenging in many cases. We therefore

used HIM-3 as a marker and measured chromosome length by tracing the length of the HIM-3 signal (Tables 3 and 4). For *hcp-6(mr17)* experiments, worms were grown at 20°C and shifted to 25°C overnight. In these conditions condensation defects were apparent, yet bivalents could be observed. For gap-size analysis (Figure 4B), we analyzed chromosomes only in "face-up position," in which clear cruciform structures could be resolved via HIM-3 staining. Any other positioning of the chromosomes obscured the gap. RNAi for *syp-2* was performed from the L1 developmental stage until 24 h post-L4 on *akir-1(gk528)/hT2* (phenotypically wild type) and *akir-1(gk528)* mutants. We assessed *akir-1(gk528)/hT2; syp-2(RNAi)* for partial depletion of SYP, as indicated by the appearance of univalents at a low frequency.

We used the following method to measure distances between DAPI bodies: a DAPI body was randomly assigned, and a distance was measured to the closest DAPI body, measuring the smallest distance between the two bodies. This analysis was continued until all DAPI bodies were used for the measurement. No DAPI body was counted more then once. Statistical comparisons between genotypes were performed using the two-tailed Mann–Whitney test.

Length of meiotic stages was measured on gonads from age-matched whole worms ethanol fixed and stained with DAPI. The length of each meiotic stage was defined by measuring the length in micrometers in the middle of the gonad of three-dimensional images. The premeiotic region was defined from the tip to the first row with clustered chromosome morphology nuclei. The transition zone was defined by the presence of rows of cells with at least one nucleus with a distinct clustered chromosome morphology. Pachytene was defined as extending from the first row after the transition zone until diplotene. Diplotene was defined as the region in which full rows of nuclei are reduced to two rows of nuclei, until the "bend" region. Diakinesis was defined as the region from the "bend" to the spermatheca.

ACKNOWLEDGMENTS

Some strains and clones were kindly provided by the *Caenorhabditis* Genetics Center and the *C. elegans* Reverse Genetics Core Facility at the University of British Columbia, which is part of the International *C. elegans* Gene Knockout Consortium. We thank M. Zetka for the HIM-3 and HTP-3 antibodies, A.F. Dernburg for the HTP1/2 antibody, R. Chan for the MIX-1 antibody, and M. Boxem for providing a cDNA library and WormBase release WS225. We thank R. Chan, G. Csankovszki, and A. Severson (Meyer lab) for providing detailed protocols for some of the experiments presented. We are grateful to R. E. Malone, B. T. Phillips, J. A. Weiner, Y. Tzur, and members of the Smolikove lab for critical reading of the manuscript. This work was supported by National Science Foundation Grant MCB-1121150 (to S.S.), a Biological Sciences Funding Program of the University of Iowa award (to S.S.), and National Institutes of Health Grant R01GM072551 (to M.P.C.).

REFERENCES

Alpi A, Pasierbek P, Gartner A, Loidl J (2003). Genetic and cytological characterization of the recombination protein RAD-51 in *Caenorhabditis elegans*. Chromosoma 112, 6–16.

Bhalla N, Wynne DJ, Jantsch V, Dernburg AF (2008). ZHP-3 acts at crossovers to couple meiotic recombination with synaptonemal complex disassembly and bivalent formation in *C. elegans*. PLoS Genet 4, e1000235.

Brenner S (1974). The genetics of *Caenorhabditis elegans*. Genetics 77, 71–94.

Carlton PM, Farruggio AP, Dernburg AF (2006). A link between meiotic prophase progression and crossover control. PLoS Genet 2, e12.

Chan RC, Severson AF, Meyer BJ (2004). Condensin restructures chromosomes in preparation for meiotic divisions. J. Cell Biol 167, 613–625.

Colaiacovo MP, MacQueen AJ, Martinez-Perez E, McDonald K, Adamo A, La Volpe A, Villeneuve AM (2003). Synaptonemal complex assembly in *C. elegans* is dispensable for loading strand-exchange proteins but critical for proper completion of recombination. Dev Cell 5, 463–474.

Cole C, Barber JD, Barton GJ (2008). The Jpred 3 secondary structure prediction server. Nucleic Acids Res 36, W197–W201.

Couteau F, Zetka M (2005). HTP-1 coordinates synaptonemal complex assembly with homolog alignment during meiosis in *C. elegans*. Genes Dev 19, 2744–2756.

Davis MW, Hammarlund M, Harrach T, Hullett P, Olsen S, Jorgensen EM (2005). Rapid single nucleotide polymorphism mapping in *C. elegans*. BMC Genomics 6, 118.

de Carvalho CE, Zaaijer S, Smolikov S, Gu Y, Schumacher JM, Colaiacovo MP (2008). LAB-1 antagonizes the Aurora B kinase in *C. elegans*. Genes Dev 22, 2869–2885.

de la Fuente R, Sanchez A, Marchal JA, Viera A, Parra MT, Rufas JS, Page J (2012). A synaptonemal complex-derived mechanism for meiotic segregation precedes the evolutionary loss of homology between sex chromosomes in arvicolid mammals. Chromosoma 121, 433–446.

Dernburg AF, McDonald K, Moulder G, Barstead R, Dresser M, Villeneuve AM (1998). Meiotic recombination in *Caenorhabditis elegans* initiates by a conserved mechanism and is dispensable for homologous chromosome synapsis. Cell 94, 387–398.

Goodyer W, Kaitna S, Couteau F, Ward JD, Boulton SJ, Zetka M (2008). HTP-3 links DSB formation with homolog pairing and crossing over during *C. elegans* meiosis. Dev Cell 14, 263–274.

Goto A, Matsushita K, Gesellchen V, El Chamy L, Kuttenkeuler D, Takeuchi O, Hoffmann JA, Akira S, Boutros M, Reichhart JM (2008). Akirins are highly conserved nuclear proteins required for NF-kappaB-dependent gene expression in *drosophila* and mice. Nat Immunol 9, 97–104.

Hassold T, Hunt P (2001). To err (meiotically) is human: the genesis of human aneuploidy. Nat Rev Genet 2, 280–291.

Hillers KJ, Villeneuve AM (2003). Chromosome-wide control of meiotic crossing over in *C. elegans*. Curr Biol 13, 1641–1647.

Hsu JY *et al.* (2000). Mitotic phosphorylation of histone H3 is governed by Ipl1/aurora kinase and Glc7/PP1 phosphatase in budding yeast and nematodes. Cell 102, 279–291.

Ivanovska I, Khandan T, Ito T, Orr-Weaver TL (2005). A histone code in meiosis: the histone kinase, NHK-1, is required for proper chromosomal architecture in *Drosophila* oocytes. Genes Dev 19, 2571–2582.

Jantsch V, Pasierbek P, Mueller MM, Schweizer D, Jantsch M, Loidl J (2004). Targeted gene knockout reveals a role in meiotic recombination for ZHP-3, a Zip3-related protein in *Caenorhabditis elegans*. Mol Cell Biol 24, 7998–8006.

Jordan P, Copsey A, Newnham L, Kolar E, Lichten M, Hoffmann E (2009). Ipl1/Aurora B kinase coordinates synaptonemal complex disassembly with cell cycle progression and crossover formation in budding yeast meiosis. Genes Dev 23, 2237–2251.

Jordan P, Karppinen J, Handel M (2012). Polo-like kinase is required for synaptonemal complex disassembly and phosphorylation in mouse spermatocytes. J Cell Sci 125, 5061–5072.

Kelly KO, Dernburg AF, Stanfield GM, Villeneuve AM (2000). *Caenorhabditis elegans* msh-5 is required for both normal and radiation-induced meiotic crossing over but not for completion of meiosis. Genetics 156, 617–630.

Komiya Y, Kurabe N, Katagiri K, Ogawa M, Sugiyama A, Kawasaki Y, Tashiro F (2008). A novel binding factor of 14–3-3beta functions as a transcriptional repressor and promotes anchorage-independent growth, tumorigenicity, and metastasis. J Biol Chem 283, 18753–18764.

MacQueen AJ, Colaiacovo MP, McDonald K, Villeneuve AM (2002). Synapsis-dependent and -independent mechanisms stabilize homolog pairing during meiotic prophase in *C. elegans*. Genes Dev 16, 2428–2442.

MacQueen AJ, Villeneuve AM (2001). Nuclear reorganization and homologous chromosome pairing during meiotic prophase require *C. elegans* chk-2. Genes Dev 15, 1674–1687.

Macqueen DJ, Johnston IA (2009). Evolution of the multifaceted eukaryotic akirin gene family. BMC Evol Biol 9, 34.

Malmanche N, Owen S, Gegick S, Steffensen S, Tomkiel JE, Sunkel CE (2007). *Drosophila* BubR1 is essential for meiotic sister-chromatid cohesion and maintenance of synaptonemal complex. Curr Biol 17, 1489–1497.

Martinez-Perez E, Schvarzstein M, Barroso C, Lightfoot J, Dernburg AF, Villeneuve AM (2008). Crossovers trigger a remodeling of meiotic chromosome axis composition that is linked to two-step loss of sister chromatid cohesion. Genes Dev 22, 2886–2901.

Martinez-Perez E, Villeneuve AM (2005). HTP-1-dependent constraints coordinate homolog pairing and synapsis and promote chiasma formation during *C. elegans* meiosis. Genes Dev 19, 2727–2743.
McKim KS, Peters K, Rose AM (1993). Two types of sites required for meiotic chromosome pairing in *Caenorhabditis elegans*. Genetics 134, 749–768.
McNally K, Audhya A, Oegema K, McNally FJ (2006). Katanin controls mitotic and meiotic spindle length. J Cell Biol 175, 881–891.
Merritt C, Rasoloson D, Ko D, Seydoux G (2008). 3′ UTRs are the primary regulators of gene expression in the *C. elegans* germline. Curr Biol 18, 1476–1482.
Mets DG, Meyer BJ (2009). Condensins regulate meiotic DNA break distribution, thus crossover frequency, by controlling chromosome structure. Cell 139, 73–86.
Miller MA, Nguyen VQ, Lee MH, Kosinski M, Schedl T, Caprioli RM, Greenstein D (2001). A sperm cytoskeletal protein that signals oocyte meiotic maturation and ovulation. Science 291, 2144–2147.
Nabeshima K, Villeneuve AM, Colaiacovo MP (2005). Crossing over is coupled to late meiotic prophase bivalent differentiation through asymmetric disassembly of the SC. J. Cell Biol 168, 683–689.
Nowak SJ, Aihara H, Gonzalez K, Nibu Y, Baylies MK (2012). Akirin links twist-regulated transcription with the Brahma chromatin remodeling complex during embryogenesis. PLoS Genet 8, e1002547.
Pasierbek P, Jantsch M, Melcher M, Schleiffer A, Schweizer D, Loidl J (2001). A *Caenorhabditis elegans* cohesion protein with functions in meiotic chromosome pairing and disjunction. Genes Dev 15, 1349–1360.
Peretz G, Arie LG, Bakhrat A, Abdu U (2009). The *Drosophila* hus1 gene is required for homologous recombination repair during meiosis. Mech Dev 126, 677–686.
Phillips CM, Wong C, Bhalla N, Carlton PM, Weiser P, Meneely PM, Dernburg AF (2005). HIM-8 binds to the X chromosome pairing center and mediates chromosome-specific meiotic synapsis. Cell 123, 1051–1063.
Resnick TD, Dej KJ, Xiang Y, Hawley RS, Ahn C, Orr-Weaver TL (2009). Mutations in the chromosomal passenger complex and the condensin complex differentially affect synaptonemal complex disassembly and metaphase I configuration in *Drosophila* female meiosis. Genetics 181, 875–887.
Rogers E, Bishop JD, Waddle JA, Schumacher JM, Lin R (2002). The aurora kinase AIR-2 functions in the release of chromosome cohesion in *Caenorhabditis elegans* meiosis. J Cell Biol 157, 219–229.
Rose AM, O'Neil NJ, Bilenky M, Butterfield YS, Malhis N, Flibotte S, Jones MR, Marra M, Baillie DL, Jones SJ (2010)Genomic sequence of a mutant strain of *Caenorhabditis elegans* with an altered recombination pattern. BMC Genomics 11, 131.
Saito TT, Youds JL, Boulton SJ, Colaiacovo MP (2009). *Caenorhabditis elegans* HIM-18/SLX-4 interacts with SLX-1 and XPF-1 and maintains genomic integrity in the germline by processing recombination intermediates. PLoS Genet 5, e1000735.
Schild-Prüfert K, Saito TT, Smolikov S, Gu Y, Hincapie M, Hill DE, Vidal M, McDonald K, Colaiacovo MP (2011). Organization of the synaptonemal complex during meiosis in *Caenorhabditis elegans*. Genetics 189, 411–421.
Schumacher JM, Golden A, Donovan PJ (1998). AIR-2: An Aurora/Ipl1-related protein kinase associated with chromosomes and midbody microtubules is required for polar body extrusion and cytokinesis in *Caenorhabditis elegans* embryos. J Cell Biol 143, 1635–1646.
Schvarzstein M, Wignall SM, Villeneuve AM (2010). Coordinating cohesion, co-orientation, and congression during meiosis: lessons from holocentric chromosomes. Genes Dev 24, 219–228.
Severson AF, Ling L, van Zuylen V, Meyer BJ (2009). The axial element protein HTP-3 promotes cohesin loading and meiotic axis assembly in *C. elegans* to implement the meiotic program of chromosome segregation. Genes Dev 23, 1763–1778.
Shakes DC, Wu JC, Sadler PL, Laprade K, Moore LL, Noritake A, Chu DS (2009). Spermatogenesis-specific features of the meiotic program in *Caenorhabditis elegans*. PLoS Genet 5, e1000611.
Smolikov S, Eizinger A, Schild-Prufert K, Hurlburt A, McDonald K, Engebrecht J, Villeneuve AM, Colaiacovo MP (2007). SYP-3 restricts synaptonemal complex assembly to bridge paired chromosome axes during meiosis in *C. elegans*. Genetics 176, 2015–2025.
Smolikov S, Schild-Prufert K, Colaiacovo MP (2008). CRA-1 uncovers a double-strand break-dependent pathway promoting the assembly of central region proteins on chromosome axes during *C. elegans* meiosis. PLoS Genet 4, e1000088.
Smolikov S, Schild-Prufert K, Colaiacovo MP (2009). A yeast two-hybrid screen for SYP-3 interactors identifies SYP-4, a component required for synaptonemal complex assembly and chiasma formation in *Caenorhabditis elegans* meiosis. PLoS Genet 5, e1000669.
Sourirajan A, Lichten M (2008). Polo-like kinase Cdc5 drives exit from pachytene during budding yeast meiosis. Genes Dev 22, 2627–2632.
Timmons L, Court DL, Fire A (2001). Ingestion of bacterially expressed dsRNAs can produce specific and potent genetic interference in *Caenorhabditis elegans*. Gene 263, 103–112.
Walker AK, Boag PR, Blackwell TK (2007). Transcription reactivation steps stimulated by oocyte maturation in *C. elegans*. Dev Biol 304, 382–393.
Wang X, Zhao Y, Wong K, Ehlers P, Kohara Y, Jones SJ, Marra MA, Holt RA, Moerman DG, Hansen D (2009). Identification of genes expressed in the hermaphrodite germ line of *C. elegans* using SAGE. BMC Genomics 10, 213.
Wignall SM, Villeneuve AM (2009). Lateral microtubule bundles promote chromosome alignment during acentrosomal oocyte meiosis. Nat Cell Biol 11, 839–844.
Zetka MC, Kawasaki I, Strome S, Muller F (1999). Synapsis and chiasma formation in *Caenorhabditis elegans* require HIM-3, a meiotic chromosome core component that functions in chromosome segregation. Genes Dev 13, 2258–2270.
Zickler D, Kleckner N (1999). Meiotic chromosomes: integrating structure and function. Annu Rev Genet 33, 603–754.